

SECTION 7

RADIATION AND RADIOLOGICAL PROTECTION

BY

JOHN M. WEST, B.S., M.S., Vice President, General Nuclear Engineering Corporation, formerly Associate Director, Reactor Engineering Division, Argonne National Laboratory.

KARL ZIEGLER MORGAN, A.B., M.A., Ph.D., Director of Health Physics Division, Oak Ridge National Laboratory.

EVERITT P. BLIZARD, B.A., M.A., Director, Applied Nuclear Physics Division, Oak Ridge National Laboratory.

RAYMOND C. GOERTZ, B.S., Director, Remote Control Engineering Division, Argonne National Laboratory.

KENNETH R. FERGUSON, A.B., M.S., Associate Physicist, Argonne National Laboratory.

WILLIAM B. DOE, B.S., Associate Chemical Engineer, Argonne National Laboratory.

CONTENTS

7-1 CALCULATION OF NUCLEAR RADIATION

BY JOHN M. WEST

	PAGE
1 Nature of Radioactivity.....	7-2
2 Transmutation by Neutrons.....	7-7
3 Fission Products.....	7-14
4 Reactor Coolant Systems.....	7-17
References.....	7-21

7-2 HEALTH PHYSICS

BY KARL ZIEGLER MORGAN

1 Ionizing Radiation.....	7-22
2 Radiation Monitoring.....	7-45
3 Decontamination.....	7-48
4 Radioactive Effluents and Wastes.....	7-50
5 Shipping and Handling of Radioactive Materials.....	7-55
6 The Safe Handling of Fuel, by Thomas J. Burnett.....	7-55
7 Beryllium Toxicity, by Myron F. Fair.....	7-57
References.....	7-57

7-3 NUCLEAR RADIATION SHIELDING

BY EVERITT P. BLIZARD

	PAGE
1 γ Ray Attenuation.....	7-61
2 Sources of γ Rays and X Rays.....	7-72
3 Neutron Attenuation Principles.....	7-78
4 Neutron Sources.....	7-90
5 Geometry.....	7-93
6 Shield Materials.....	7-109
References.....	7-115

7-4 MECHANICAL HANDLING OF RADIOACTIVE MATERIALS

BY RAYMOND C. GOERTZ, KENNETH R. FERGUSON, and WILLIAM B. DOE

1 General Solutions to Handling Problems.....	7-117
2 Typical Equipment for Handling Radioactive Materials.....	7-125
References.....	7-139

7-1 CALCULATION OF NUCLEAR RADIATION

BY

John M. West

1 NATURE OF RADIOACTIVITY

1.1 Radioactivity

Nuclei which spontaneously undergo atomic disintegration by emitting particles or electromagnetic radiation are said to be radioactive.

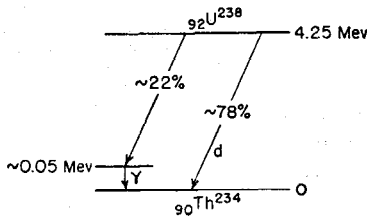
1.11 Natural Radioactivity. Unstable nuclei which exist in nature are said to be naturally radioactive. In addition to certain individual radioactive isotopes such as K^{40} there are three major decay chains. The isotope of uranium having a mass of 238 (U^{238}) is the first member of a chain which, after emitting eight α particles and six β particles, terminates as a stable isotope of lead (Pb^{206}). Similar chains begin with U^{235} and thorium (Th^{232}) and terminate as Pb^{206} and Pb^{208} . The three natural radioactive chains are referred to as the uranium-radium, uranium-actinium, and thorium families,^{1*} respectively.

1.12 Induced Radioactivity. When a nucleus is made to react with a particle or electromagnetic radiation to form an unstable nucleus which did not previously exist in nature, the new atom is said to be artificially radioactive.

1.13 Decay Mechanisms. In their approach to a stable state, radioactive atoms may emit charged particles of various types (α particles, β particles, positrons), uncharged particles (neutrons), or electromagnetic radiation (γ rays, X rays).

Alpha Decay. The α particle is identical with the nucleus of a helium atom. The emission of an α particle creates a new nucleus with an atomic number reduced by 2 and an atomic weight decreased by four mass units.

Alpha decay is common in the three natural radioactive chains. The mechanism by which U^{238} decays to Th^{234} follows:†



It should be noted that the α ray may be emitted in either of two ways. The 4.20-Mev α is emitted followed by a 0.05-Mev γ ray about 22 per cent of the time. In the remaining 78 per cent of the transitions, the full energy difference between U^{238} and Th^{234} is carried away by the 4.25-Mev particle.

Beta Decay. In β decay a negative electron is emitted from the nucleus of an atom. Since atomic number is defined by the net positive charge of the nucleus, ejection of a β ray increases the atomic number by unity. Gamma rays are usually emitted also to carry away excess energy of the new nucleus. An example follows:‡

* Superscript numbers refer to References at end of subsection.

† See Ref. 2, p. 607.

‡ See Ref. 2, p. 482.

7-3 NUCLEAR RADIATION SHIELDING

BY

Everitt P. Blizard

The primary purpose of shields is to protect personnel and equipment outside a reactor from the radiations that are produced inside. In addition, of course, other radioactive sources must be shielded as well. The shield which protects personnel is referred to as the biological shield. Many layers of material are usually placed between the reactive core itself and the outside of the shield, and all these attenuate the radiation and must be taken account of in a shield design. Accordingly, the shield actually consists of all the material between the source of radiation and the occupied regions. Of these layers, several might be named. The first is the reflector, the prime purpose of which is to "reflect" or scatter neutrons back into the reactive core. Next might be the first part of the shield proper. At the inside of the shield there is often considerable heat deposited by the radiation. In order to ensure that this heat is removed and does not cause damage to other regions beyond it, a special section, called a *thermal shield*, is usually installed. This shield might typically be a slab of iron cooled by water or gas. Following the thermal shield might be a pressure shell, to contain radioactive fission products, coolant, etc. Finally, the biological shield proper would follow, which in many stationary installations consists of concrete, either ordinary or of some special aggregate such as barytes or limonite. This section discusses the whole complex of layers outside the reactive core and the means by which the required radiation attenuation is produced.

The section is divided into several articles, the first of which deals with that information which is best known, namely, γ -ray attenuation theory. Methods are described for calculating the attenuation of radiation from a point source as measured by a point detector at some distance in an infinite homogeneous medium. In Art. 2 the γ -ray sources are listed and described. Article 3 discusses the neutron attenuation theory, again for a point source and point detector in infinite homogeneous media, with the neutron sources described in Art. 4. In Art. 5, on geometry, the extension from point sources to actual large distributions of sources such as reactors is described, and practical problems are treated in terms of the simple attenuation calculations of Arts. 1 and 3. Article 6 deals with shield materials, giving information on materials which have been of common interest in attenuation problems.

The theory of γ -ray attenuation in single media is well understood, and answers are available for all energies and thicknesses of interest. For multiple regions the theory is considerably less clear. For the case of neutron attenuation in hydrogenous shields, such as water, there is a theory which agrees reasonably well with experiment. Inhomogeneities in the shield, as with layers of different materials, make the problems of calculating either neutron or γ -ray attenuation so difficult as to be essentially unsolved by the more sophisticated techniques. Even mixtures of materials present problems that cannot be simply solved at this time. As a consequence of this, much of the shielding lore in this handbook appears as rules of thumb or laws which have been developed simply because they describe reasonably well the phenomena which have been observed in measurements. The solutions are not satisfactory in the sense that they give exact answers. Nevertheless, the accuracy which is required in shield design is not great, and it is possible to design shields with sufficient accuracy for most conditions.

1 GAMMA-RAY ATTENUATION^{*1-3}

1.1 Attenuation Processes

The attenuation of γ rays in matter is attributable primarily to three processes by which their energy is given to electrons. These electrons slow down quickly, producing heat in the immediate vicinity. The processes are described below.

1.11 Photoelectric Effect. The γ -ray photon gives all its energy to an atom, causing the ejection of an electron from an orbit (usually an inner orbit). The ensuing X ray caused by readjustment of electrons in the atom is usually replaced by emission of a second "Auger" electron. As a result the photoelectric effect can be accurately treated as an absorption process. The photoelectric-effect cross section varies from element to element approximately as Z^5 (Z is the atomic number). It is the dominant process for low-energy photons and materials of high atomic number Z . (It dominates for energies less than 150 kev with copper and for energies less than 500 kev for lead.)

1.12 Pair Production. The photon creates a positron-electron pair and is absorbed in the process. The positron subsequently is annihilated nearby, giving two photons of 0.51 Mev. Since these are not very penetrating in comparison with the original photon, they are usually assumed to be absorbed nearby, so that the pair-production process is treated effectively as an absorption process. It does not occur for photons of energy below 1.02 Mev, and it increases in cross section with increasing photon energy. It varies from element to element as Z^2 . It is the dominant effect for high-energy photons and high-atomic-number materials (i.e., it is dominant for $E > 80$, 15, or 5 Mev, with materials of $Z = 1, 13$, or 82, respectively).

1.13 Compton Effect. The photon interacts with an atomic electron, which is loosely bound in the sense that its binding energy is small compared with that of the photon, giving some energy to the electron and proceeding with lower energy and altered course. The probability for scattering through any angle varies with primary photon energy, the scattering being more forward for the higher photon energies. The energy E' of the scattered photon is uniquely determined by the initial energy E and the scattering angle θ as follows:

$$E' = \frac{E}{1 + (1 - \cos \theta)(E/0.51 \text{ Mev})} \quad (1)$$

where all energies are expressed in million electron volts. For small scattering angles the degradation in energy is least. The cross section is also greatest for this case. For 90° scattering, the scattered photon can have no more than 0.51 Mev regardless of the initial energy. For 180° scattering (back scattering), the scattered photon can have no more than 0.255 Mev. The cross section for the Compton effect varies from element to element directly with Z . It decreases with increasing photon energy but is the dominant effect in the intermediate energy region. Because of the Compton-scattered photons the attenuation in matter is effectively decreased, a fact which is taken account of by the so-called "build-up factor" in attenuation calculations.

1.2 Attenuation Coefficients

The attenuation coefficients are quantities which indicate the attenuation by all three of the foregoing processes.

1.21 The total linear attenuation coefficient μ is the sum of the macroscopic cross sections for all three processes. Thus the current density of uncollided photons at a distance from a point source of photons is

$$\Gamma^0(R,t) = \frac{Se^{-\mu t}}{4\pi R^2} \text{ photons}/(\text{cm}^2)(\text{sec}) \quad (2)$$

* Superscript numbers refer to References at end of subsection.

Table 1. Total Mass Attenuation Coefficients μ/ρ , cm²/g
(Ref. 4)

Mat'l	Energy, Mev																	
	0.1	0.15	0.2	0.3	0.4	0.5	0.6	0.8	1.0	1.25	1.5	2	3	4	5	6	8	10.0
H	0.295	0.265	0.243	0.212	0.189	0.173	0.160	0.140	0.126	0.113	0.103	0.0876	0.0691	0.0579	0.0502	0.0446	0.0371	0.0321
Be	0.132	0.119	0.109	0.0945	0.0847	0.0773	0.0715	0.0628	0.0565	0.0504	0.0459	0.0394	0.0313	0.0266	0.0234	0.0211	0.0180	0.0161
C	0.149	0.134	0.122	0.106	0.0953	0.0870	0.0805	0.0707	0.0636	0.0568	0.0518	0.0444	0.0356	0.0304	0.0270	0.0245	0.0213	0.0194
N	0.150	0.134	0.123	0.106	0.0955	0.0869	0.0805	0.0707	0.0636	0.0568	0.0517	0.0445	0.0357	0.0306	0.0273	0.0249	0.0218	0.0200
O	0.151	0.134	0.123	0.107	0.0953	0.0870	0.0806	0.0708	0.0636	0.0568	0.0518	0.0445	0.0359	0.0309	0.0276	0.0254	0.0224	0.0206
Na	0.151	0.130	0.118	0.102	0.0912	0.0833	0.0770	0.0676	0.0608	0.0546	0.0496	0.0427	0.0348	0.0303	0.0274	0.0254	0.0229	0.0215
Mg	0.160	0.135	0.122	0.106	0.0944	0.0860	0.0795	0.0699	0.0627	0.0560	0.0512	0.0442	0.0360	0.0315	0.0286	0.0266	0.0242	0.0228
Al	0.161	0.134	0.120	0.103	0.0922	0.0840	0.0777	0.0683	0.0614	0.0548	0.0500	0.0432	0.0353	0.0310	0.0282	0.0264	0.0241	0.0229
Si	0.172	0.139	0.125	0.107	0.0954	0.0869	0.0802	0.0706	0.0635	0.0567	0.0517	0.0447	0.0367	0.0323	0.0296	0.0277	0.0254	0.0243
P	0.174	0.137	0.122	0.104	0.0928	0.0846	0.0780	0.0685	0.0617	0.0551	0.0502	0.0436	0.0358	0.0316	0.0290	0.0273	0.0252	0.0242
S	0.188	0.144	0.127	0.108	0.0958	0.0874	0.0806	0.0707	0.0635	0.0568	0.0519	0.0448	0.0371	0.0328	0.0302	0.0284	0.0266	0.0255
A	0.188	0.135	0.117	0.0977	0.0867	0.0790	0.0730	0.0638	0.0573	0.0512	0.0468	0.0407	0.0338	0.0301	0.0279	0.0266	0.0248	0.0241
K	0.215	0.149	0.127	0.106	0.0938	0.0852	0.0786	0.0689	0.0618	0.0552	0.0505	0.0438	0.0365	0.0327	0.0305	0.0289	0.0274	0.0267
Ca	0.238	0.158	0.132	0.109	0.0965	0.0876	0.0809	0.0708	0.0634	0.0566	0.0518	0.0451	0.0376	0.0338	0.0316	0.0302	0.0285	0.0280
Fe	0.344	0.183	0.138	0.106	0.0919	0.0828	0.0762	0.0664	0.0595	0.0531	0.0485	0.0424	0.0361	0.0330	0.0313	0.0304	0.0295	0.0294
Cu	0.427	0.206	0.147	0.108	0.0916	0.0820	0.0751	0.0654	0.0585	0.0521	0.0476	0.0418	0.0357	0.0330	0.0316	0.0309	0.0303	0.0305
Mo	1.03	0.389	0.225	0.130	0.0998	0.0851	0.0761	0.0648	0.0575	0.0510	0.0467	0.0414	0.0365	0.0349	0.0344	0.0344	0.0349	0.0359
Sn	1.58	0.563	0.303	0.153	0.109	0.0886	0.0776	0.0647	0.0568	0.0501	0.0459	0.0408	0.0367	0.0355	0.0355	0.0358	0.0368	0.0383
I	1.83	0.648	0.339	0.165	0.114	0.0913	0.0792	0.0653	0.0571	0.0502	0.0460	0.0409	0.0370	0.0360	0.0361	0.0365	0.0377	0.0394
W	4.21	1.44	0.708	0.293	0.174	0.125	0.101	0.0763	0.0640	0.0544	0.0492	0.0437	0.0405	0.0402	0.0409	0.0418	0.0438	0.0465
Pt	4.75	1.64	0.795	0.324	0.191	0.135	0.107	0.0800	0.0659	0.0554	0.0501	0.0445	0.0414	0.0411	0.0418	0.0427	0.0448	0.0477
Tl	5.16	1.80	0.866	0.346	0.204	0.143	0.112	0.0824	0.0675	0.0563	0.0508	0.0452	0.0420	0.0416	0.0423	0.0433	0.0454	0.0484
Pb	5.29	1.84	0.896	0.356	0.208	0.145	0.114	0.0836	0.0684	0.0569	0.0512	0.0457	0.0421	0.0420	0.0426	0.0436	0.0459	0.0489
U	1.06	2.42	1.17	0.452	0.259	0.176	0.136	0.0952	0.0757	0.0615	0.0548	0.0484	0.0445	0.0440	0.0446	0.0455	0.0479	0.0511
Air	0.151	0.134	0.123	0.106	0.0953	0.0868	0.0804	0.0706	0.0635	0.0567	0.0517	0.0445	0.0357	0.0307	0.0274	0.0250	0.0220	0.0202
NaI	1.57	0.568	0.305	0.155	0.111	0.0901	0.0789	0.0657	0.0577	0.0508	0.0465	0.0412	0.0367	0.0351	0.0347	0.0347	0.0354	0.0366
H ₂ O	0.167	0.149	0.136	0.118	0.106	0.0966	0.0896	0.0786	0.0706	0.0630	0.0575	0.0493	0.0396	0.0339	0.0301	0.0275	0.0240	0.0219
Concrete*	0.169	0.139	0.124	0.107	0.0954	0.0870	0.0804	0.0706	0.0635	0.0567	0.0517	0.0445	0.0363	0.0317	0.0287	0.0268	0.0243	0.0229
Tissue†	0.163	0.144	0.132	0.115	0.100	0.0936	0.0867	0.0761	0.0683	0.0600	0.0556	0.0478	0.0384	0.0329	0.0292	0.0267	0.0233	0.0212

* Ordinary concrete: 0.56 per cent H, 49.5 per cent O, 31.35 per cent Si, 4.56 per cent Al, 8.26 per cent Ca, 1.22 per cent Fe, 0.24 per cent Mg, 1.71 per cent Na, 1.92 per cent K, 0.12 per cent S by weight.

† Tissue is material of the average composition of man.

Table 2. Energy Absorption Mass Attenuation Coefficients, μ_a/ρ , cm²/g*
(Calculated from Ref. 4)

Mat'l	Energy, Mev																	
	0.1	0.15	0.2	0.3	0.4	0.5	0.6	0.8	1.0	1.25	1.50	2	3	4	5	6	8	10.0
H	0.0411	0.0487	0.0531	0.0575	0.0589	0.0591	0.0590	0.0575	0.0557	0.0533	0.0509	0.0467	0.0401	0.0354	0.0318	0.0291	0.0252	0.0255
Be	0.0183	0.0217	0.0237	0.0256	0.0263	0.0264	0.0263	0.0256	0.0248	0.0237	0.0227	0.0210	0.0183	0.0164	0.0151	0.0141	0.0127	0.0118
C	0.0215	0.0246	0.0267	0.0288	0.0296	0.0297	0.0296	0.0289	0.0280	0.0268	0.0256	0.0237	0.0209	0.0190	0.0177	0.0166	0.0153	0.0145
N	0.0224	0.0249	0.0267	0.0288	0.0296	0.0297	0.0296	0.0289	0.0280	0.0268	0.0256	0.0238	0.0211	0.0193	0.0180	0.0171	0.0158	0.0151
O	0.0233	0.0252	0.0271	0.0289	0.0296	0.0297	0.0296	0.0289	0.0280	0.0268	0.0257	0.0238	0.0212	0.0195	0.0183	0.0175	0.0163	0.0157
Na	0.0289	0.0258	0.0266	0.0279	0.0283	0.0284	0.0284	0.0276	0.0268	0.0257	0.0246	0.0229	0.0207	0.0194	0.0185	0.0179	0.0171	0.0168
Mg	0.0335	0.0276	0.0278	0.0290	0.0294	0.0293	0.0292	0.0285	0.0276	0.0265	0.0254	0.0237	0.0215	0.0203	0.0194	0.0188	0.0182	0.0180
Al	0.0373	0.0283	0.0275	0.0283	0.0287	0.0286	0.0286	0.0278	0.0270	0.0259	0.0248	0.0232	0.0212	0.0200	0.0192	0.0188	0.0183	0.0182
Si	0.0435	0.0300	0.0286	0.0291	0.0293	0.0290	0.0290	0.0282	0.0274	0.0263	0.0252	0.0236	0.0217	0.0206	0.0198	0.0194	0.0190	0.0189
P	0.0501	0.0315	0.0292	0.0289	0.0290	0.0290	0.0287	0.0280	0.0271	0.0260	0.0250	0.0234	0.0216	0.0206	0.0200	0.0197	0.0194	0.0195
S	0.0601	0.0351	0.0310	0.0301	0.0301	0.0300	0.0298	0.0288	0.0279	0.0268	0.0258	0.0242	0.0224	0.0215	0.0209	0.0206	0.0206	0.0206
A	0.0729	0.0368	0.0302	0.0278	0.0274	0.0272	0.0270	0.0260	0.0252	0.0242	0.0233	0.0220	0.0206	0.0199	0.0195	0.0195	0.0194	0.0197
K	0.0909	0.0433	0.0340	0.0304	0.0298	0.0295	0.0291	0.0282	0.0272	0.0261	0.0251	0.0237	0.0222	0.0217	0.0214	0.0212	0.0215	0.0219
Ca	0.111	0.0489	0.0367	0.0318	0.0309	0.0304	0.0300	0.0290	0.0279	0.0268	0.0258	0.0244	0.0230	0.0225	0.0222	0.0223	0.0225	0.0231
Fe	0.225	0.0810	0.0489	0.0340	0.0307	0.0294	0.0287	0.0274	0.0261	0.0250	0.0242	0.0231	0.0224	0.0224	0.0227	0.0231	0.0239	0.0250
Cu	0.310	0.107	0.0594	0.0368	0.0316	0.0296	0.0286	0.0271	0.0260	0.0247	0.0237	0.0229	0.0223	0.0227	0.0231	0.0237	0.0248	0.0261
Mo	0.922	0.294	0.141	0.0617	0.0422	0.0348	0.0315	0.0281	0.0263	0.0248	0.0239	0.0233	0.0237	0.0250	0.0262	0.0274	0.0296	0.0316
Sn	1.469	0.471	0.222	0.0873	0.0534	0.0403	0.0346	0.0294	0.0268	0.0248	0.0239	0.0233	0.0243	0.0259	0.0276	0.0291	0.0316	0.0339
I	1.726	0.557	0.260	0.100	0.0589	0.0433	0.0366	0.0303	0.0274	0.0252	0.0241	0.0236	0.0247	0.0265	0.0283	0.0299	0.0327	0.0353
W	4.112	1.356	0.631	0.230	0.121	0.0786	0.0599	0.0426	0.0353	0.0302	0.0281	0.0271	0.0287	0.0311	0.0335	0.0355	0.0390	0.0426
Pt	4.645	1.556	0.719	0.262	0.138	0.0892	0.0666	0.0465	0.0375	0.0315	0.0293	0.0280	0.0296	0.0320	0.0343	0.0365	0.0400	0.0438
Pb	5.057	1.717	0.791	0.285	0.152	0.0972	0.0718	0.0491	0.0393	0.0326	0.0301	0.0288	0.0304	0.0326	0.0349	0.0354	0.0406	0.0446
Tl	5.193	1.753	0.821	0.294	0.156	0.0994	0.0738	0.0505	0.0402	0.0332	0.0306	0.0293	0.0305	0.0330	0.0352	0.0373	0.0412	0.0450
U	0.963	2.337	1.096	0.392	0.208	0.132	0.0968	0.0628	0.0482	0.0383	0.0346	0.0324	0.0332	0.0352	0.0374	0.0394	0.0443	0.0474
Air	0.0233	0.0251	0.0268	0.0288	0.0296	0.0297	0.0296	0.0289	0.0280	0.0268	0.0256	0.0238	0.0211	0.0194	0.0181	0.0172	0.0160	0.0153
NaI	1.466	0.476	0.224	0.0889	0.0542	0.0410	0.0354	0.0299	0.0273	0.0253	0.0242	0.0235	0.0241	0.0254	0.0268	0.0281	0.0303	0.0325
H ₂ O	0.0253	0.0278	0.0300	0.0321	0.0328	0.0330	0.0329	0.0321	0.0311	0.0298	0.0285	0.0264	0.0233	0.0213	0.0198	0.0188	0.0173	0.0165
Concrete†	0.0416	0.0300	0.0289	0.0294	0.0297	0.0296	0.0295	0.0287	0.0278	0.0272	0.0256	0.0239	0.0216	0.0203	0.0194	0.0188	0.0180	0.0177
Tissue‡	0.0271	0.0282	0.0293	0.0312	0.0317	0.0320	0.0319	0.0311	0.0300	0.0288	0.0276	0.0256	0.0220	0.0206	0.0192	0.0182	0.0168	0.0160

* Photoelectric and pair production interactions assumed to be pure absorption.

† Ordinary concrete: 0.56 per cent H, 49.5 per cent O, 31.35 per cent Si, 4.56 per cent Al, 8.26 per cent Ca, 1.22 per cent Fe, 0.24 per cent Mg, 1.71 per cent Na, 1.92 per cent K, 0.12 per cent S by weight.

‡ Tissue is material of the average composition of man.

where

S = source strength, photons/sec

R = distance from source, cm

μ = probability per unit distance for interaction, or the macroscopic cross section, for all processes in the material, cm^{-1} (Table 1 gives values of μ/ρ , where ρ = density, g/cm^3 , for the material and for the photon energy E_0 , of the source)

= $\mu_{pe} + \mu_c + \mu_{pp}$

t = thickness of attenuating material, cm

μ_{pe} , μ_c , and μ_{pp} = macroscopic cross sections for photoelectric effect, Compton effect, and pair production, respectively

The uncollided flux from a collimated plane source incident on a shield of thickness x is

$$\Gamma^o(x) = \Gamma^o(0)e^{-\mu x} \quad (2a)$$

where $\Gamma^o(0)$ is the incident flux.

1.22 The energy-absorption linear attenuation coefficient μ_a is the probability for interaction, per unit distance traversed, multiplied by the average fractional energy loss on interaction. In common usage the energy loss on Compton scatterings is assumed to be the difference in photon energy pre- and postscattering, but all energy is assumed lost on photoelectric and pair-production interactions.

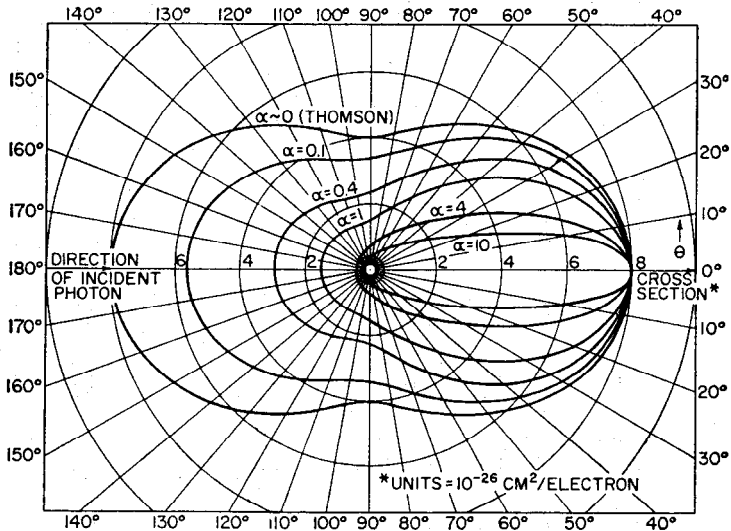


Fig. 1. Differential Compton cross section for scattering by electrons of photons of energy $\alpha m_0 c^2$ ($m_0 c^2 = 0.51$ Mev) through any angle θ , in units of 10^{-26} $\text{cm}^2/\text{electron}/\text{sterad}$. (Ref. 5.)

1.23 Mass attenuation coefficients are the foregoing quantities μ , μ_a divided by the material density ρ . Since the linear attenuation coefficient is clearly proportional to the quantity of material traversed in a given distance, the mass attenuation coefficients are independent of the material density, being dependent only upon the energy of the γ rays and the type of material. It is for this reason that the mass attenuation coefficients for the different elements are given in the tables. Table 1 gives the *total mass attenuation coefficients*, and Table 2 gives the *energy absorption mass attenuation coefficients*. Figure 1 gives the differential Compton cross section for scattering of photons through any angle. Figure 2 gives the same quantity multiplied by the fractional energy carried away by the scattered photon.⁵

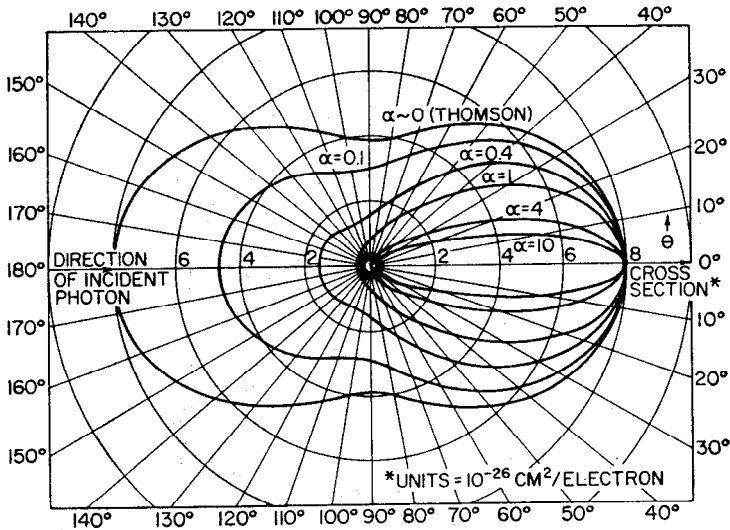


FIG. 2. Differential Compton cross section for scattering by electrons of photons of energy $\alpha m_0 c^2$ ($m_0 c^2 = 0.51$ Mev), through any angle θ , multiplied by the ratio of scattered to incident photon energy, in units of 10^{-26} cm²/electron/sterad. (Ref. 5, p. 83.)

1.3 Gamma-ray Dose Rate and Heating Data

1.31 Units of Radiation Dose. Physical radiation dose is measured in terms of the energy deposition. The unit is the "rad," which is the quantity of radiation which deposits 100 ergs per gram of material. Physical radiation dose has been measured also in rep (roentgens equivalent physical), where 1 rep = 0.93 rad for the case in which the rads are measured in air.

Biological radiation dose is measured in terms of the biological effect of X rays (usually with those produced at 250 kv). The factor by which the physical radiation dose in tissue must be multiplied to obtain the biological quantity is called the relative biological effectiveness (RBE). The RBE will vary with the biological effect being studied. The unit of biological dose is the rem (rad equivalent, man). The RBE is currently taken to be 1.0 for all X rays and γ rays. This factor may change as better information is obtained.

1.32 Calculation of γ -ray Dose. The current density of unscattered photons from a single isotropic point source is given by Eq. (2). The dose rate which the unscattered radiation induces is given by

$$D^\circ(R) = 5.767 \times 10^{-6} \frac{\mu_a}{\rho} E_\sigma \Gamma^\circ(R,t) \text{ rads/hr} \tag{3}$$

where E_σ = photon energy of radiation source, Mev

μ_a/ρ = energy-absorption mass attenuation coefficient for the source energy and the material in which dose is to be calculated, cm²/g (Table 2).

Unless otherwise specified, dose in air is usually implied, although dose in tissue is more nearly the desired quantity. The two are about the same

$\Gamma^\circ(R,t)$ = current density of unscattered photons, summed or integrated over all sources, photons/(cm²)(sec), as calculated by Eq. (2)

Since most dose-rate calculations are for tissue, Table 3 is supplied which gives the conversion factors in Eq. (3) as a function of photon energy in a convenient form.

The dose rate from scattered plus unscattered photons due to a point source is given by

$$D_r(R,t) = B_r(\mu t) D^\circ(R,t) \text{ rads/hr} \tag{4}$$

Table 3. Flux for Unit Tissue Dose*

E_0 , photon energy, Mev	Photon flux for 1 rad/hr, $\text{cm}^{-2} \text{sec}^{-1}$	Energy flux for 1 rad/hr, $\text{Mev}/(\text{cm}^2)(\text{sec})$
0.10	5.90×10^8	5.90×10^8
0.15	3.88×10^8	5.82×10^8
0.20	2.91×10^8	5.82×10^8
0.30	1.847×10^8	5.54×10^8
0.40	1.357×10^8	5.43×10^8
0.50	1.085×10^8	5.425×10^8
0.60	9.065×10^7	5.44×10^8
0.90	6.98×10^7	5.58×10^8
1.0	5.77×10^7	5.77×10^8
1.25	4.77×10^7	5.96×10^8
1.5	4.18×10^7	6.27×10^8
2.0	3.405×10^7	6.81×10^8
3.0	2.63×10^7	7.89×10^8
4.0	2.10×10^7	8.41×10^8
5.0	1.80×10^7	9.00×10^8
6.0	1.577×10^7	9.46×10^8
8.0	1.278×10^7	1.022×10^9
10.0	1.067×10^7	1.067×10^9

* Calculated from Ref. 4.

where $B_r(\mu t)$ is the dose-rate build-up factor chosen from Tables 4 and 5 for source energy E_0 per photon, material of shield, thickness of shield t , attenuation coefficient μ for source energy E_0 , and geometry (point isotropic or plane collimated source—see below).

For more complicated source configurations it is necessary to integrate this expression over the sources, since doses from different sources must be added to obtain total dose at a point.

The build-up factors in Tables 4 and 5 are calculated on the assumption that the dose is to be determined in air. They are adequate for dose in tissue, since the mass attenuation coefficients are very nearly the same.

For convenience, Table 6 is given, which shows the number of curies of Co^{60} and Cs^{137} γ -ray sources which are adequately shielded in lead shields of different thicknesses.

1.33 Calculations of Heating Due to γ Rays. The rate of heat deposition in the shield from scattered plus unscattered γ radiation at a distance R from the source with t cm of shield intervening is given by

$$H(R,t) = 1.602 \times 10^{-6} \frac{\mu_a}{\rho} E_0 B_a(\mu t) \Gamma^2(R,t) \quad \text{ergs}/(\text{sec})(\text{g}) \quad (5)$$

where $B_a(\mu t)$ = energy absorption build-up factor, chosen for photon energy E_0 , material, and number of relaxation lengths in the shield μt (Table 7)
 μ_a/ρ = energy absorption mass attenuation coefficient for the shield material, cm^2/gm (from Table 2)

1.4 Factors Affecting Computational Method

The use of the foregoing article and the accompanying tables is dependent upon the conditions of the problem. In most instances a judicious choice must be made with some compromise in accuracy. The recommendations which follow are designed to give conservative estimates of dose rate with a minimum of complication. More sophisticated approaches yielding more accurate results can be found in the references.

1.41 Choice of "Point Isotropic" (Table 4) or "Plane Collimated" (Table 5) Build-up Factors. If the source is embedded in or immediately adjacent to the shield, the "point isotropic" build-up factor is to be used (Fig. 3a). If a small (in linear extent)

Table 4. Dose Build-up Factor, B_r
(Point isotropic source, Ref. 2)

Material	E_0 , Mev	μ							
		1	2	4	7	10	15	20	
Water.....	0.255	3.09	7.14	23.0	72.9	166	456	982	
	0.5	2.52	5.14	14.3	38.8	77.6	178	334	
	1.0	2.13	3.71	7.68	16.2	27.1	50.4	82.2	
	2.0	1.83	2.77	4.88	8.46	12.4	19.5	27.7	
	3.0	1.69	2.42	3.91	6.23	8.63	12.8	17.0	
	4.0	1.58	2.17	3.34	5.13	6.94	9.97	12.9	
	6.0	1.46	1.91	2.76	3.99	5.18	7.09	8.85	
	8.0	1.38	1.74	2.40	3.34	4.25	5.66	6.95	
	10.0	1.33	1.63	2.19	2.97	3.72	4.90	5.98	
	Aluminum..	0.5	2.37	4.24	9.47	21.5	38.9	80.8	141
1.0		2.02	3.31	6.57	13.1	21.2	37.9	58.5	
2.0		1.75	2.61	4.62	8.05	11.9	18.7	26.3	
3.0		1.64	2.32	3.78	6.14	8.65	13.0	17.7	
4.0		1.53	2.08	3.22	5.01	6.88	10.1	13.4	
6.0		1.42	1.85	2.70	4.06	5.49	7.97	10.4	
8.0		1.34	1.68	2.37	3.45	4.58	6.56	8.52	
10.0		1.28	1.55	2.12	3.01	3.96	5.63	7.32	
Iron.....		0.5	1.98	3.09	5.98	11.7	19.2	35.4	55.6
		1.0	1.87	2.89	5.39	10.2	16.2	28.3	42.7
	2.0	1.76	2.43	4.13	7.25	10.9	17.6	25.1	
	3.0	1.55	2.15	3.51	5.85	8.51	13.5	19.1	
	4.0	1.45	1.94	3.03	4.91	7.11	11.2	16.0	
	6.0	1.34	1.72	2.58	4.14	6.02	9.89	14.7	
	8.0	1.27	1.56	2.23	3.49	5.07	8.50	13.0	
	10.0	1.20	1.42	1.95	2.99	4.35	7.54	12.4	
	Tin.....	0.5	1.56	2.08	3.09	4.57	6.04	8.64	
		1.0	1.64	2.30	3.74	6.17	8.85	13.7	18.8
2.0		1.57	2.17	3.53	5.87	8.53	13.6	19.3	
3.0		1.46	1.96	3.13	5.28	7.91	13.3	20.1	
4.0		1.38	1.81	2.82	4.82	7.41	13.2	21.2	
6.0		1.26	1.57	2.37	4.17	6.94	14.8	29.1	
8.0		1.19	1.42	2.05	3.57	6.19	15.1	34.0	
10.0		1.14	1.31	1.79	2.99	5.21	12.5	33.4	
Tungsten..		0.5	1.28	1.50	1.84	2.24	2.61	3.12	
		1.0	1.44	1.83	2.57	3.62	4.64	6.25	(7.35)*
	2.0	1.42	1.85	2.72	4.09	5.27	8.07	(10.6)*	
	3.0	1.36	1.74	2.59	4.00	5.92	9.66	14.1	
	4.0	1.29	1.62	2.41	4.03	6.27	12.0	20.9	
	6.0	1.20	1.43	2.07	3.60	6.29	15.7	36.3	
	8.0	1.14	1.32	1.81	3.05	5.40	15.2	41.9	
	10.0	1.11	1.25	1.64	2.62	4.65	14.0	39.3	
	Lead.....	0.5	1.24	1.42	1.69	2.00	2.27	2.65	(2.73)*
		1.0	1.37	1.69	2.26	3.02	3.74	4.81	5.86
2.0		1.39	1.76	2.51	3.66	4.84	6.87	9.00	
3.0		1.34	1.68	2.43	3.75	5.30	8.44	12.3	
4.0		1.27	1.56	2.25	3.61	5.44	9.80	16.3	
5.1		1.21	1.46	2.08	3.44	5.55	11.7	23.6	
6.0		1.18	1.40	1.97	3.34	5.69	13.8	32.7	
8.0		1.14	1.30	1.74	2.89	5.07	14.1	44.6	
10.0		1.11	1.23	1.58	2.52	4.34	12.5	39.2	
Uranium...		0.5	1.17	1.30	1.48	1.67	1.85	2.08	
	1.0	1.31	1.56	1.98	2.50	2.97	3.67		
	2.0	1.33	1.64	2.23	3.09	3.95	5.36	(6.48)*	
	3.0	1.29	1.58	2.21	3.27	4.51	6.97	9.88	
	4.0	1.24	1.50	2.09	3.21	4.66	8.01	12.7	
	6.0	1.16	1.36	1.85	2.96	4.80	10.8	23.0	
	8.0	1.12	1.27	1.66	2.61	4.36	11.2	28.0	
	10.0	1.09	1.20	1.51	2.26	3.78	10.5	28.5	

* Extrapolated values.

Table 5. Dose Build-up Factor, B_r
(Plane collimated source, Ref. 2)

Material	E_0 , Mev	μR					
		1	2	4	7	10	15
Water.....	0.5	2.63	4.29	9.05	20.0	35.9	74.9
	1.0	2.26	3.39	6.27	11.5	18.0	30.8
	2.0	1.84	2.63	4.28	6.96	9.87	14.4
	3.0	1.69	2.31	3.57	5.51	7.48	10.8
	4.0	1.58	2.10	3.12	4.63	6.19	8.54
	6.0	1.45	1.86	2.63	3.76	4.86	6.78
	8.0	1.36	1.69	2.30	3.16	4.00	5.47
	10.0	1.22	1.44	1.95	2.89	4.07	6.70
Iron.....	0.5	2.07	2.94	4.87	8.31	12.4	20.6
	1.0	1.92	2.74	4.57	7.81	11.6	18.9
	2.0	1.69	2.35	3.76	6.11	8.78	13.7
	3.0	1.58	2.13	3.32	5.26	7.41	11.4
	4.0	1.48	1.90	2.95	4.61	6.46	9.92
	6.0	1.35	1.71	2.48	3.81	5.35	8.39
	8.0	1.27	1.55	2.17	3.27	4.58	7.33
	10.0	1.22	1.44	1.95	2.89	4.07	6.70
Tin.....	1.0	1.65	2.24	3.40	5.18	7.19	10.5
	2.0	1.58	2.13	3.27	5.12	7.13	11.0
	4.0	1.39	1.80	2.69	4.31	6.30	11.0
	6.0	1.27	1.57	2.27	3.72	5.77	9.68
	10.0	1.16	1.33	1.77	2.81	4.53	9.68
Lead.....	0.5	1.24	1.39	1.63	1.87	2.08	4.20
	1.0	1.38	1.68	2.18	2.80	3.40	4.20
	2.0	1.40	1.76	2.41	3.36	4.35	5.94
	3.0	1.36	1.71	2.42	3.55	4.82	7.18
	4.0	1.28	1.56	2.18	3.29	4.69	7.70
	6.0	1.19	1.40	1.87	2.97	4.69	9.53
	8.0	1.14	1.30	1.69	2.61	4.18	9.08
	10.0	1.11	1.24	1.54	2.27	3.54	7.70
Uranium.....	0.5	1.17	1.28	1.45	1.60	1.73	3.60
	1.0	1.30	1.53	1.90	2.32	2.70	3.60
	2.0	1.33	1.62	2.15	2.87	3.56	4.89
	3.0	1.29	1.57	2.13	3.02	3.99	5.94
	4.0	1.25	1.49	2.02	2.94	4.06	6.47
	6.0	1.18	1.37	1.82	2.74	4.12	7.79
	8.0	1.13	1.27	1.61	2.39	3.65	7.36
	10.0	1.10	1.21	1.48	2.12	3.21	6.58

Table 6. Lead Shield Thicknesses for Co^{60} and Cs^{137} Sources

Lead thickness, in.	Activity, curies	
	Co^{60}	Cs^{137}
1	1.4×10^{-5}	1.3×10^{-4}
2	1.9×10^{-4}	7.5×10^{-3}
3	1.7×10^{-3}	2.5×10^{-1}
4	1.3×10^{-2}	6.4
5	9×10^{-2}	1.6×10^2
6	6×10^{-1}	3.7×10^3
8	2.3×10^1	2×10^4
10	8×10^2	8×10^5
12	3×10^4	
14	8×10^5	
16	2.3×10^7	
18	7×10^8	

These shields are presumed to be spherical with the source near the inside surface. The dose at the outer surface will be 7.5 mrem/hr, which is laboratory tolerance.

source is far from the shield, so that the radiation is nearly collimated, use the "plane collimated" build-up factor (Fig. 3b). In case the sources are spread over a large surface near the shield but not on it, an integration must be made over the surface (Fig. 3c).

In order to decide whether, in this integration over the array of sources, the point isotropic or plane collimated build-up factor is to be used, it is necessary to define

Table 7. Energy-absorption Build-up Factor, B^a
(Point isotropic source, Ref. 2)

Material	E_0 , Mev	μt						
		1	2	4	7	10	15	20
Water.....	0.255	3.03	6.88	21.8	68.1	154	421	906
	0.5	2.46	4.93	13.4	36.1	71.5	163	306
	1.0	2.13	3.71	7.85	16.8	28.2	51.9	83.8
	2.0	1.85	2.82	4.99	8.67	12.9	20.0	28.6
	3.0	1.74	2.52	4.10	6.57	9.12	13.4	17.9
	4.0	1.59	2.18	3.37	5.18	7.01	10.1	13.0
	6.0	1.46	1.89	2.76	3.98	5.18	7.07	8.83
	8.0	1.38	1.74	2.42	3.36	4.28	5.70	7.00
	10.0	1.31	1.60	2.13	2.88	3.60	4.73	5.76
Aluminum..	0.5	2.61	4.92	11.4	26.9	49.2	104	185
	1.0	2.15	3.64	7.40	15.0	23.2	44.1	69.1
	2.0	1.80	2.74	4.93	8.63	12.8	20.2	28.3
	3.0	1.66	2.37	3.88	6.35	8.94	13.4	18.2
	4.0	1.54	2.09	3.24	5.05	6.93	10.2	13.5
	6.0	1.40	1.81	2.63	3.92	5.27	7.62	9.92
	8.0	1.31	1.62	2.26	3.25	4.28	6.10	7.88
	10.0	1.25	1.51	2.02	2.83	3.70	5.22	6.74
	Iron.....	0.5	2.80	4.84	9.97	20.4	34.2	64.3
1.0		2.19	3.58	7.00	13.6	21.9	38.8	58.5
2.0		1.78	2.64	4.53	7.90	11.9	19.3	27.4
3.0		1.58	2.21	3.61	6.05	8.82	14.0	19.8
4.0		1.45	1.95	3.03	4.90	7.10	11.1	16.7
6.0		1.30	1.63	2.38	3.73	5.35	8.67	12.7
8.0		1.21	1.45	1.99	2.99	4.23	6.89	10.4
10.0		1.16	1.35	1.78	2.61	3.69	6.17	9.89
Tin.....		0.5	2.25	3.38	5.51	8.58	11.6	17.0
	1.0	2.12	3.18	5.47	9.31	13.6	21.3	28.7
	2.0	1.73	2.54	4.35	7.48	11.0	17.7	24.1
	3.0	1.49	2.03	3.30	5.62	8.43	15.2	20.2
	4.0	1.34	1.74	2.67	4.47	6.80	13.2	19.1
	6.0	1.21	1.45	2.06	3.47	5.38	10.9	20.8
	8.0	1.14	1.31	1.74	2.73	4.38	9.70	20.8
	10.0	1.11	1.24	1.58	2.38	3.78	8.81	20.3
	Lead.....	0.5	1.51	1.80	2.19	2.61	3.01	3.52
1.0		1.76	2.37	3.39	4.74	6.01	7.78	9.70
2.0		1.58	2.10	3.14	4.70	6.32	9.05	12.0
3.0		1.37	1.73	2.50	3.85	5.43	8.65	12.6
4.0		1.24	1.49	2.09	3.25	4.79	8.46	13.9
5.11		1.19	1.39	1.89	2.96	4.61	9.38	18.5
6.0		1.14	1.29	1.70	2.63	4.20	9.46	21.5
8.0		1.10	1.21	1.50	2.21	3.50	8.60	23.0
10.0		1.08	1.16	1.38	1.92	2.92	7.15	20.4

the principal cone of radiation. This cone, the apex of which is at the outer shield surface, includes all rays through the shield for which $\mu l \leq \mu t + 1$, l being the shield thickness, μ the attenuation coefficient, and l the ray length in the shield. Plane collimated build-up factors are then used if all the radiation incident on the shield within the base of this cone arrives at an angle to the shield normal no greater than

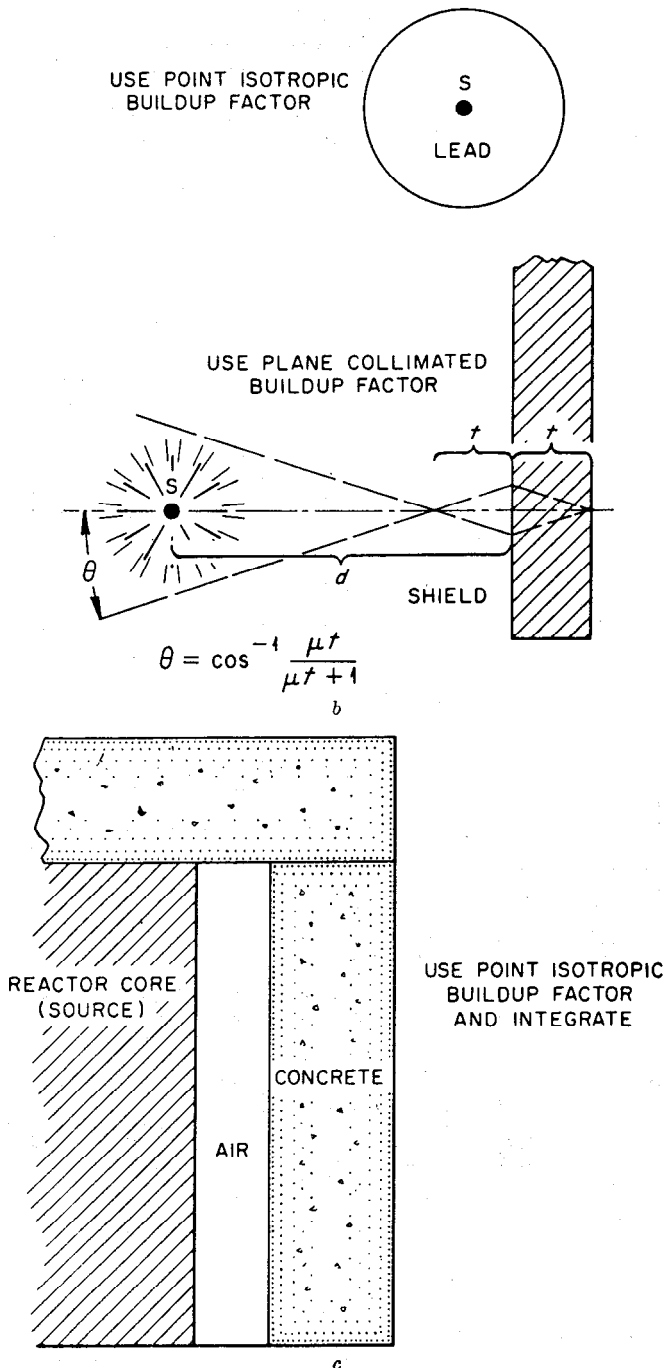


FIG. 3. a. Geometry for case of source in shield. b. Geometry for case of source far away from shield. c. Geometry for case of large source near shield.

the cone half angle. In other words, if

$$\frac{a}{d-t} < \frac{\sqrt{2\mu t + 1}}{\mu t}$$

and $d > t$, use plane collimated build-up factors. (Otherwise point isotropic build-up factors are to be used.)

where d = distance from source array to shield

a = maximum radius of source array, measured perpendicular to d

t = shield thickness

1.42 Attenuation Coefficient for Single Element Not Listed in Tables. Since the tables cover most elements commonly used in shields, this should not often be a problem. However, the quantities $A\mu/\rho$ and $A\mu_a/\rho$ (A = atomic weight) are smooth functions of the atomic number Z . Plot the values of this quantity for neighboring elements against Z , and interpolate.

1.43 Build-up Factor for Element Not Listed in Tables. Build-up factors are smooth functions of atomic number Z . Interpolate.

1.44 Attenuation Coefficient for Homogeneous or Nearly Homogeneous Shield of Many Elements. Number the elements in the shield 1, 2, 3, . . . , i , . . . , n .

Determine the fractional densities ρ_i for each element (shield density $\rho = \sum_i \rho_i$)

and the attenuation coefficients $(\mu/\rho)_i$. The attenuation coefficient (either kind) is determined by summation as follows:

$$\frac{\mu}{\rho}, \text{ shield} = \frac{1}{\rho} \sum_i \left(\frac{\mu}{\rho}\right)_i \rho_i \quad (6)$$

Example:

$$\frac{\mu}{\rho}, \text{ H}_2\text{O}, 1 \text{ Mev} = \frac{1}{1} (0.126 \times 0.11 + 0.0636 \times 0.89) = 0.0706 \text{ cm}^2/\text{g}$$

1.45 Build-up Factor for Homogeneous or Nearly Homogeneous Shield of Many Elements. There is no simple way to choose the build-up factor for this case from among the tables available here. If a conservative but not necessarily accurate answer is required, choose the build-up factor for the component which would give the largest dose rate. Calculate the number of mean free paths μt , using the method of the foregoing paragraph. If a more accurate result is needed, plot μ/ρ for the shield material vs. photon energy E for all energies below the source energy and choose an element for which the same plot is similar in shape. Use the build-up factors as if the shield were wholly of this element.

1.46 Attenuation Coefficient for Laminated Shield. Number the layers 1, 2, . . . , j , . . . , m . Determine the attenuation coefficients $(\mu/\rho)_j$ for these layers and their thicknesses t_j . The exponent μt in Eq. (2) for calculating Γ° , the unscattered current density, is replaced by a summation as follows:

$$\mu t = \sum_j \left(\frac{\mu}{\rho}\right)_j \rho_j t_j \quad (7)$$

Note that empty regions in a shield are taken account of in this expression, since the density will be zero or nearly so, nullifying their contribution to the exponential attenuation, although the geometric attenuation $1/R^2$ will be unaffected.

1.47 Build-up Factor for Laminated Shield. Build-up factors have not been calculated for laminated shields. However, the build-up factor is largely determined by the total number of mean free paths (μt , from previous paragraph) and is characteristic of the material in the outermost region if this is at least two or three mean free paths in thickness $\{(\mu/\rho)t \rho > 2\}$. Choose the build-up factor for the material of the outermost thick region and for the number of mean free paths in the whole shield (μt). In case the outermost single region is not thick, use the method of Art. 1.45 above, for the materials constituting the outermost two or three mean free paths.

2 SOURCES OF γ RAYS AND X RAYS

Gamma rays are produced in nuclear transitions. X rays come from atomic rearrangement or from electron acceleration in the atomic coulomb field. Except for their origins they are indistinguishable. Sources of γ rays in reactor installations are discussed below.

2.1 Prompt-fission γ Rays

At the moment of fission, γ rays are given off from the fissioning nucleus. The total energy given off is 7.46 Mev per fission^{6,7} on the average. Similarly there are

Table 8. Energy Spectrum of Prompt γ Rays from Fission of U²³⁵*

γ -ray energy, Mev	γ rays per 0.1 Mev	γ -ray energy, Mev	γ rays per 0.1 Mev	γ -ray energy, Mev	γ rays per 0.1 Mev
		2.7	0.0409	5.3	0.00399
0.2	0.815	2.8	0.0369	5.4	0.00371
0.3	0.697	2.9	0.0330	5.5	0.00341
0.4	0.661	3.0	0.0298	5.6	0.00314
0.5	0.622	3.1	0.0268	5.7	0.00290
0.6	0.553	3.2	0.0244	5.8	0.00264
0.7	0.474	3.3	0.0219	5.9	0.00243
0.8	0.408	3.4	0.0198	6.0	0.00223
0.9	0.353	3.5	0.0181	6.1	0.00204
1.0	0.307	3.6	0.0165	6.2	0.00188
1.1	0.272	3.7	0.0150	6.3	0.00172
1.2	0.240	3.8	0.0136	6.4	0.00157
1.3	0.205	3.9	0.0126	6.5	0.00139
1.4	0.180	4.0	0.0116	6.6	0.00128
1.5	0.158	4.1	0.0106	6.7	0.00115
1.6	0.139	4.2	0.00985	6.8	0.00103
1.7	0.125	4.3	0.00908	6.9	0.000916
1.8	0.113	4.4	0.00830	7.0	0.000833
1.9	0.102	4.5	0.00764	7.1	0.000731
2.0	0.0907	4.6	0.00704	7.2	0.000629
2.1	0.0818	4.7	0.00649	7.3	0.000547
2.2	0.0726	4.8	0.00604	7.4	0.000467
2.3	0.0651	4.9	0.00556	7.5	0.000388
2.4	0.0579	5.0	0.00519	7.6	0.000308
2.5	0.0512	5.1	0.00470		
2.6	0.0457	5.2	0.00430		

* R. L. Gamble, "Prompt Fission Gamma Rays from Uranium 235," Dissertation, University of Texas, Austin, Tex., June, 1955.

7.51 photons per fission on the average. The energy per photon is distributed according to Table 8. A simple analytic form for this distribution, good to ± 30 per cent in the region from 0.2 to 7 Mev, is

$$Y(E) = 7.5e^{-E} \quad (8)$$

where $Y(E)$ = number of photons given off per Mev energy interval at energy E
 E = photon energy, Mev

It is to be noted that no γ rays are reported of energy greater than 7.6 Mev.

2.2 Decay γ Rays from Fission Products

Most fission products are radioactive, emitting β and γ rays. Both the fission products and their emanations are tabulated elsewhere.⁸ The radiations from gross fission products vary widely in energy and the decays are of various half-lives. A quite complete analysis by Clark⁹ has been used⁹ to obtain plots of γ -ray emanation

in million electron volts per second per watt, for seven energy groups. Some of this data is reproduced as Fig. 4. The figure gives the energy release, in million electron volts per second per watt, produced by U^{235} fission products for infinitely long periods of operation. Thus, if $\Gamma_i(T_0, T_d)$ is the energy release rate in million electron volts per second per watt for the i th energy group at T_d days after shutdown, following T_0 days of reactor operation or fissioning, the ordinate of the figure gives

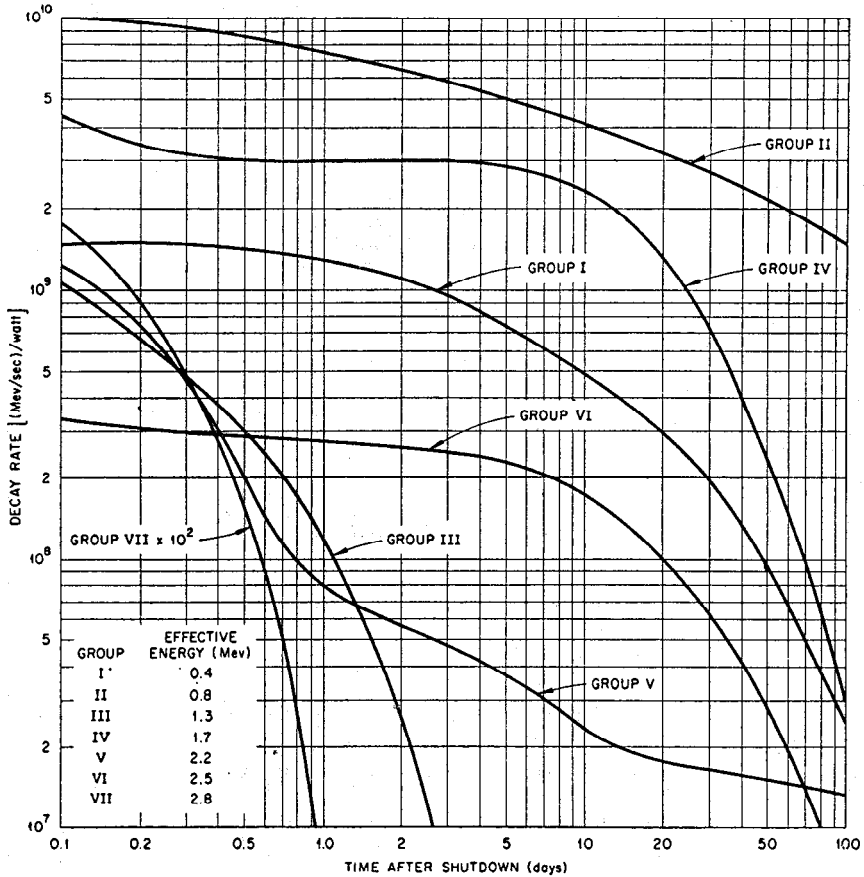


FIG. 4. Decay of fission products after infinite operation.

$\Gamma_i(\infty, T_d)$. For any other operation time the energy release rate can be found by the following relation:

$$\Gamma_i(T_0, T_d) = \Gamma_i(\infty, T_d) - \Gamma_i(\infty, T_0 + T_d) \tag{9}$$

2.3 Decay γ Rays from Activated Materials

Decay γ rays originate in activated reactor structure, shielding, housing, etc. Many elements, upon absorbing neutrons, become radioactive and decay with the release of β or γ rays or both. The data (cross sections, decay rates, and energies) on these activations are given in the chart of the isotopes.¹⁰ See also Table 20 of Sec. 1-1.

Table 9. Gamma Rays from Thermal Neutron Capture

Target	Thermal (n, γ) cross section, barns	Spectral type	Photons in designated energy intervals per 100 captures, Mev					Highest energy γ ray, Mev	Average No. photons/ capture ²⁴	Fraction of energy emitted $S(E_m)^{10a}$		References	Decay $\gamma^{b,c}$
			0-1	1-3	3-5	5-7	> 7			E_m Mev	$S(E_m)$		
Aluminum	0.215	1	?	>13	77	21	35	7.724	~2	2.5	0.78	2	2.3-min Al ²⁸ : 100(1.80) Complicated Complicated, uncertain
Antimony	6.4	3d	?	~80	36	12	6.80	2.7	2.5	0.78	13		
Arsenic	4.1	3d	?	~80	47	22	7.30				13		
Barium	1.17	3d	?	~80	75	14	9.23	4.1	2.5	0.78	14		
Beryllium ^e	0.009	1	0	0	50	75	0				6.814	9	
Bismuth ^e	0.015	1	0	0	100	0	0	4.17	26	0.78	1		
Boron-10 ^f	3,990	4	0	0	0	0	0	0.478			6, 14, 17,		
Cadmium	3,500	3d	>120	20	73	17	1	9.046	4.1	2.5	0.78	20-23, 28, 29, 37	
Cadmium-113	25,000		123	>44								36	
Calcium	0.406	2	?	50	60	101	2.4	7.83	2.6	0.80	3, 16		
Carbon-12	0.0045	1	?	<30	100	0	0	4.95	1.3	3.68	0.93	8, 9	
Chlorine	32	2	?	20	13	18	21	8.56	3.1	3.3	0.26	3, 15, 21, 22, 28, 29, 31, 37	
Chromium	2.9	1d	>37	16	12	18	69	9.716	>2	2.8	0.73	4, 16, 27	
Cobalt	34.8	2d	?	?	36	49	8	7.486	2.5	0.67		5, 7, 21, 22, 27	
Copper	3.59	1d	?	?	>23	22	42	7.914	2.6	3.4	0.67	5, 7, 27	
Fluorine	0.009	1	?	?	?	35	0	6.63	3.9	3.4	0.67	4	
Gadolinium	36,300	3d	?	80	23	4	2	7.78				14	
Gold	94	3d	?	?	66	38	0	6.494	3.5			13, 17, 27	
Hydrogen-1 ^e	0.330	1	0	100	0	0	0	2.230				25, 30	
Indium	190	3d	?	?	36	4	0	5.86	3.3			13	
Iodine	6.1	3	Many	?	?	?	?	7.0 ± 0.4				27, 38	
Iron	2.43	1d	?	<10	24	22	50	10.16	1.7	3.0	0.78	4, 27, 33	
Lead ^e	0.17	1	0	0	0	7	93	7.38				1	
Lithium-6	930	4	0	0	0	0	0	0				26	
Magnesium	0.059	2	?	>59	110	25	11	9.216	2.6	0.99		2, 11, 16	
Manganese	12.6	2d	?	?	>27	30	27	7.261	2.6	3.5	0.64	5, 7, 19, 27, 32	
Mercury	380	3d	?	?	86	41	0	6.446	3.3			14	
Molybdenum	2.4	3d	?	?	84	26	3	9.15				14	
Nickel	4.8	1	?	?	>14	30	72	8.997	3.4	0.95		4	
												54.3-min In ¹¹⁴ : 18(2.09), 15(1.49), 54(1.27), 39(1.09)	
												5.3-year Co ⁶⁰ : 100(1.17), 100(1.33)	
												12-sec F ²⁰ : 100(1.63)	
												9.58-min Mg ²⁷ : 10(0.84), 2(1.01) 2.59-hr Mn ⁵⁴ : 100(0.845), 25(1.81), 15(2.13)	

Table 9. Gamma Rays from Thermal Neutron Capture. (Continued)

Target	Thermal (n, γ) cross section, barns	Spectral type	Photons in designated energy intervals per 100 captures, Mev					Highest energy γ ray, Mev	Average No. photons/capture ²⁴	Fraction of energy emitted $S(E_m)^{10a}$		References	Decay γ s ^{b,c}
			0-1	1-3	3-5	5-7	>7			E_m Mev	$S(E_m)$		
Niobium	1.1	3d	?	?	54	14	0	7.19	2.6			13	
Nitrogen-14	0.1	2, 4	?	<5	<35	90	39	10.8				8	
Phosphorus	0.193	2	?	?	115	43	11	7.94	2.5	0.66		3	
Platinum	8.1	3d	?	~120	45	15	1	7.920				14	Complicated
Potassium	1.89	2	?	?	36	32	12	9.28	3.00	0.48		3, 12, 16	
Praseodymium	11.2	3d	?	~80	34	8	0	5.83				13	19-hr Pr ¹⁴² : 4(1.58)
Rhodium	150	3d	?	~70	38	10	0	6.792				13	Exist (34)
Samarium	10,600	3d	?	~150	45	5	1	7.89	5.6			14	
Scandium	22	3d	?	?	63	29	14	8.85				5, 7	85-day Sc ⁴⁶ : 100(1.12), 100(0.89)
Selenium	11.8	3d	?	?	65	27	11	10.483				14	
Silicon	0.160	2	?	>100	229	41	16	10.55		2.5	1.44	2, 16	
Silver	60	3d	?	~90	70	17	0.5	7.27	2.9			13	Complicated 270-day Ag ¹¹⁰
Sodium	0.47	2	?	>50	61	29	0	6.41	<2			2, 15, 17, 37	14.9-hr Na ²⁴ : 100(2.758), 100(1.380)
Strontium	1.16	(2-3)d	?	~140	62	49	13	9.22				14	
Sulphur	0.49	2	?	>19	80	91	8	8.64		2.7	0.76	3	
Talantum	21.3	3d	?	~50	26	2	0	6.07				13	Complicated
Thallium	3.3	3d	?	~100	76	62	0	6.54				13	
Tin	0.65	3d	?	?	139	33	4	9.35				14	
Titanium	5.8	2d	>50	100	33	99	10	9.39		2.4	1.02	4, 15, 18, 27	
Tungsten	19.2	3d	?	?	53	14.5	0.5	7.42				14	
Vanadium-51	4.7	3d	?	?	24	54	18	7.305	2.5	2.6	0.82	5, 7, 27	3.74-min V ⁵² : 100(1.46)
Zinc	1.06	(2-3)d	?	?	48	29	17	9.51		2.8	0.60	4	250-day Zn ⁶⁵ : 25(1.12)
Zirconium ^d	0.18	3d	?	?	113	35	4	8.66				14	65-day Zr ⁸⁵ : ~98(0.750), 35-day Nb ⁸⁵ : 100(0.764)

7-75

^a Fraction S of available energy emitted by γ rays with energy greater than E_m . E_m is the minimum γ -ray energy observed in the measurement; it has no deep significance.

^b "Complicated" means that decay γ s above 750 keV are claimed to exist but the multiplicity of isotopes and/or the complexity of the decay schemes render estimations of intensities difficult. See Ref. 33 for data.

^c Notation for decay γ rays is as follows: Half-life of decay- γ emitter is given first, then number of decay γ rays of each energy >750 keV per 100 neutron captures. Energy is in parentheses. Thus "9.58-min Mg²⁷: 10(0.84), 2(1.01)" means isotope emits 10 0.84- and 2 1.01-MeV decay γ rays per 100 captures.

^d For elements thus marked, number of unresolved photons has been determined; for all others only the intensity of resolved lines is given.

^e For these elements, the highest energy γ ray is the only γ ray present in the highest occupied energy interval. For lead, in addition, the seven 5- to 7-MeV γ rays are all 6.73 MeV; for beryllium, in addition, the fifty 3- to 5-MeV γ s are all 3.37 MeV.

^f Boron-10 decay γ is from Li⁷ following α decay of B¹¹.

^g Capture- γ -ray intensities for zirconium may be off by 50 per cent.

Table 9. Gamma Rays from Thermal Neutron Capture. (References)

1. B. B. Kinsey, G. A. Bartholomew, and W. H. Walker, *Phys. Rev.*, **82**: 380 (1950).
 2. B. B. Kinsey, G. A. Bartholomew, and W. H. Walker, *Phys. Rev.*, **83**: 519 (1951).
 3. B. B. Kinsey, G. A. Bartholomew, and W. H. Walker, *Phys. Rev.*, **85**: 1012 (1952).
 4. B. B. Kinsey and G. A. Bartholomew, *Phys. Rev.*, **89**: 375 (1953).
 5. G. A. Bartholomew and B. B. Kinsey, *Phys. Rev.*, **89**: 386 (1953).
 6. G. A. Bartholomew and B. B. Kinsey, *Phys. Rev.*, **90**: 355A (1953).
 7. G. A. Bartholomew and B. B. Kinsey, *Phys. Rev.*, **93**: 1434(E) (1954).
 8. B. B. Kinsey, G. A. Bartholomew, and W. H. Walker, *Can. J. Phys.*, **29**: 1 (1951).
 9. G. A. Bartholomew and B. B. Kinsey, *Can. J. Phys.*, **31**: 49 (1953).
 10. B. B. Kinsey and G. A. Bartholomew, *Can. J. Phys.*, **31**: 537 (1953).
 11. B. B. Kinsey and G. A. Bartholomew, *Can. J. Phys.*, **31**: 901 (1953).
 12. G. A. Bartholomew and B. B. Kinsey, *Can. J. Phys.*, **31**: 927 (1953).
 13. G. A. Bartholomew and B. B. Kinsey, *Can. J. Phys.*, **31**: 1025 (1953).
 14. B. B. Kinsey and G. A. Bartholomew, *Can. J. Phys.*, **31**: 1051 (1953).
 15. T. H. Braid, *Nuclear Sci. Abstr.*, **7**, No. 6B, New Nuclear Data (1953); *Phys. Rev.*, **90**: 355A (1953).
 16. T. H. Braid, *Phys. Rev.*, **91**: 442 (1953).
 17. H. T. Motz, *Phys. Rev.*, **90**: 355A (1953), *Nuclear Science Abstracts*, **7**, No. 6B, New Nuclear Data (1953).
 18. H. T. Motz, *Phys. Rev.*, **93**: 925A (1954).
 19. R. W. Pringle and G. Isford, *Phys. Rev.*, **83**: 467 (1951).
 20. R. W. Pringle, *Phys. Rev.*, **87**: 1016 (1952).
 21. W. A. Reardon, R. W. Krone, and R. Stump, *Phys. Rev.*, **91**: 334 (1953).
 22. W. A. Reardon, R. W. Krone, and R. Stump, *Phys. Rev.*, **91**: 442A (1953).
 23. W. Thornton, et al., *Phys. Rev.*, **86**: 604A (1952).
 24. C. O. Muehlhause, *Phys. Rev.*, **79**: 277 (1950).
 25. R. E. Bell, L. G. Elliot, *Phys. Rev.*, **79**: 282 (1950).
 26. F. Ajzenberg and T. Lauritsen, *Revs. Mod. Phys.*, **27**: 77 (1955).
 27. M. Reier and M. H. Shamos, *Phys. Rev.*, **95**: 636A (1954), also *Phys. Rev.*, **100**: 1302 (1955).
 28. A. Reicksiedler and B. Hamermesh, *Phys. Rev.*, **95**: 650 (1954).
 29. A. Reicksiedler and B. Hamermesh, *Phys. Rev.*, **96**: 109 (1954).
 30. B. Hamermesh and R. J. Culp, *Phys. Rev.*, **92**: 211L (1953).
 31. B. Hamermesh and V. Hummel, *Phys. Rev.*, **88**: 916 (1952).
 32. B. Hamermesh and V. Hummel, *Phys. Rev.*, **83**: 663 (1951).
 33. J. M. Hollander, I. Perlman, and G. T. Seaborg, *Revs. Mod. Phys.*, **25**: 469 (1953).
 34. P. Chudom and C. O. Muehlhause, Plutonium Project Report CP-3801, p. 25.
 35. "Neutron Cross Section," AECU-2040.
 36. H. T. Motz, *Phys. Rev.*, **99**: 656A (1955).
 37. C. H. Millur, A. G. W. Cameron, and M. Glicksman, *Can. J. Research*, **A28**: 475 (1950).
 38. H. E. Kubitschek and S. M. Dancoff, *Phys. Rev.*, **76**: 531 (1949).
- source: P. S. Mittleman and R. A. Liedtke, *Nucleonics*, **13**(5): 50 (1955), revised and brought up to date as of April, 1956.

2.4 Capture γ Rays

At the instant of neutron capture (within $\sim 10^{-14}$ sec), the capturing nucleus gives off γ rays of total energy equal to the neutron binding energy. (Subsequently, radioactive decay γ rays may be emitted, often much later.) Since all neutrons which do not cause fission or other nuclear reactions are captured, this source is very strong—the most important single source of γ rays from the point of view of shielding. Table 9 gives the yields for capture by various elements.¹¹ Elements may be classed as capture γ -ray emitters according to the distribution of energy among the emitted photons. For all (n, γ) reactions, the total energy of all photons emitted for one capture is just equal to the binding energy. The types are as follows:

Type 1: Essentially all energy in a single photon of maximum or near-maximum energy.

Type 2: Spectrum shows many γ -ray energies possible, with distinct line structure evident.

Type 3: Spectrum shows many γ -ray energies possible, with no line structure evident below 5 Mev. Generally softer radiation than from Type 2.

Type 4: Decay by charged-particle emission, e.g., (n, α) or (n, p) (see Table 10). Li^6 reacts wholly by (n, α) , giving no γ ray. B^{10} gives a single 0.48-Mev γ ray in 93 per cent of neutron absorptions. In 94 per cent of absorptions N^{14} gives no γ rays but releases a proton instead; in 5.6 per cent of absorptions, the proton plus recoiling $\text{C}^{14}(\text{n} + \text{N}^{14} \rightarrow \text{p} + \text{C}^{14})$ have 0.624 Mev.

Table 10. Nuclei Useful in Suppression of Capture γ Rays

Target nucleus	Reaction	Thermal-neutron cross section, barns		Energy release, Q, Mev
		Natural element	Isotope	
Li^6	$\text{Li}^6(n, \alpha)\text{H}^3$	70	930	4.78
B^{10}	$\text{B}^{10}(n, \alpha)\text{Li}^7$	50	266	2.792
	$\text{B}^{10}(n, \alpha)\text{Li}^7 + 0.48\text{-Mev } \gamma$	700	3,720	2.792
N^{14}	$\text{N}^{14}(n, p)\text{C}^{14}$	1.68	1.68	0.624
	$\text{N}^{14}(n, \gamma)\text{N}^{15}$	0.1	0.1	10.8

Suppression of capture γ rays can be accomplished by introduction of class 4 nuclei, for which capture γ rays are nonexistent, of low energy, or appreciably less frequently produced. Nuclei suitable for these purposes are given in Table 10.

2.5 Inelastic Scattering γ Rays

Fast neutrons, on scattering inelastically from nuclei, give some of their kinetic energy to the struck nucleus in the form of intrinsic nuclear energy. The neutrons proceed with altered course and lower energy. The nucleus at once gives up the intrinsic energy by emission of one or more γ -ray photons. The available energy will be distributed among the photons according to the energy levels available to the nucleus in the readjustment process, that is, to the nuclear levels between that to which the nucleus is excited by neutron impact and the ground state. The Nuclear Cross Section Committee is collecting and publishing data on inelastic scattering γ -ray production as they become available.¹² Both cross sections and photon energy distributions are required for shielding calculations, so the compilation of that committee is needed. In the absence of such data, it is, of course, conservative to assume that all neutron energy is given to the struck nucleus and that a single photon carries it off (see also Art. 3.22).

2.6 X Rays

Characteristic X rays are produced following photoelectric interaction of γ rays or other processes in which the atomic electrons are disturbed. These X rays are, in general, soft and of negligible consequence in reactor shield design.

Continuous X rays, or bremsstrahlung, are produced when a high-energy electron is deflected in the coulomb field of a nucleus.¹³ This is the common process by which X rays are produced in commercial machines. The only case in which this is of significance in reactors is that of Li⁷ coolant. The reaction $\text{Li}^7(n, \gamma)\text{Li}^8$, for which the thermal-neutron cross section is 0.033 barn, gives Li⁸, which decays with a half-life of 0.88 sec, yielding a β ray of maximum energy 13.1 Mev. This β ray is sufficiently energetic to produce appreciable X rays by the bremsstrahlung process.

3 NEUTRON ATTENUATION PRINCIPLES

Neutron shielding is not at present so well understood as is that of γ rays, so that greater safety factors are called for. In general, best estimates of shield thickness should be increased by 10 per cent to ensure adequate attenuation in those cases in which a full-thickness shield cannot be tested experimentally.

The method to be described of calculating neutron shielding differs from that of the preceding article on γ rays, in that the build-up factor is not taken as a separate factor. Instead, the scattered neutrons are taken into account by using cross sections somewhat lower than the measured total cross sections. This is tantamount to using build-up factors which are exponential in mathematical form. This approach ignores such questions as the order in which materials may appear in a laminated shield, but no reliable theory is available to cope with these problems with the brevity required here. The recommended safety factor (10 per cent in thickness) should suffice for this shortcoming, provided the recommendations regarding configuration are adhered to.

3.1 Neutron Sources in a Reactor*

The dominant source of neutrons in a reactor is the fission process itself. On fission, U²³⁵ gives 2.5 neutrons on the average, distributed in energy from near 0 to about 17 Mev, approximately according to the empirical formula of Watt:

$$N(E) = \sqrt{\frac{2}{\pi e}} e^{-E} \sinh \sqrt{2E} \quad (10)$$

where $N(E)$ = probability (normalized to one) that a virgin fission neutron will have energy E Mev, per unit Mev energy interval

E = neutron energy, Mev

This function, plus integrals above and below a given energy, are given in Table 15.

There are several things to note about this spectrum of neutrons: The most probable energy is about $\frac{3}{4}$ Mev; the average energy per neutron is about 2 Mev. Above this energy, the neutrons become increasingly less frequently produced, and at energies as high as 15 Mev there are extremely few neutrons. Most reactors contain a large quantity of low-atomic-weight material which serves as a moderator to reduce the energy of the neutrons within the reactor. Some reactors also include a reflector which, likewise, usually reduces the average energy of the neutrons. The result is that there is, in general, a large number of low-energy neutrons entering the shield and a small number of high-energy neutrons. The low-energy neutrons are usually captured in the first layers of the shield, giving rise to a large γ -ray source in this region. The high-energy neutrons, on the other hand, are more penetrating, and the bulk of the biological shield is required to stop this component.

In addition to the prompt fission neutrons just described, there are delayed neutrons which are emitted by the fission products themselves. These delayed neutrons have half-lives ranging from a few seconds to many minutes. The delayed neutrons can

* See also Art. 4 on Neutron Sources.

be characterized as belonging to a set of individual radioactive emitters, each having a characteristic energy spectrum and half-life. The delayed neutron emitters give neutron spectra which are peaked approximately at the energies shown in Table 16.

The delayed neutrons are appreciably lower in energy than the prompt fission neutrons, and it is evident from the recent work of investigators at the Atomic Energy Research Establishment at Harwell, England, that there are no very high neutron energies among the delayed neutrons.

3.2 Neutron Attenuation Processes

3.21 Elastic Scattering. In this process the neutrons are changed in direction and reduced somewhat in energy. For heavy nuclei, the reduction in energy is insignificant; for hydrogen, the reduction in energy is one-half of the initial energy, on the average; for high-energy neutrons of several Mev or greater, the elastic scattering is dominantly in the forward direction; that is to say, the change in direction occasioned by elastic scattering is, on the average, not very great. For this reason, the elastic scattering process is not so effective in attenuation as might be otherwise thought. Elastic scattering in hydrogen is an exception to this because of the large energy degradation it introduces.

3.22 Inelastic Scattering. For neutrons of energies greater than about 1 Mev it is possible for the struck nucleus to be raised to an excited state by transfer of some of the kinetic energy of the neutron to the intrinsic nuclear energy of the struck particle. This process is nonexistent for hydrogen but relatively quite probable for the larger nuclei. It is very effective in reducing the energy of the neutron, but it gives rise to inelastic scattering γ rays which are produced when the excited nucleus returns to the ground state. The emission of the inelastic scattering γ rays occurs essentially immediately following the neutron collision. These inelastic scattering γ rays constitute an additional hazard which must be taken into account in the design of the reactor shield.

3.23 Capture (n, γ). All neutrons which do not undergo particle reactions such as (n, α) or (n, p) with nuclei are eventually captured. The cross section for this process is, however, significant only for low neutron energies. There is some capture in the resonant region, that is, at about 100 kv or less, and there is, in general, very strong capture for thermal neutrons in most materials. The most pronounced exceptions are He, Be, C, O, F, Mg, and Bi. Immediately following neutron capture, γ rays are given off with total energy equal to the binding energy of the extra neutron in the new nucleus. For hydrogen, this energy is 2.23 Mev; for most other nuclei it is of the order of 7 Mev. These new γ rays constitute an additional source of radiation against which shielding must be provided. In some nuclei only a single capture γ ray is given off, and this is then a very hard or penetrating γ ray. In other nuclei many γ rays are given off, and since the total energy is just equal to the binding energy of the neutron, they are of lower energy per photon. It is almost never necessary to add a material to a shield to ensure neutron capture. Almost all elements have sufficient thermal-neutron capture cross section to ensure that neutrons which are sufficiently reduced in energy will be captured before traveling very far. Exceptions to this include the materials of interest for moderators or reflectors in reactor cores, such as beryllium or graphite. These are seldom used in biological shields in any case, although as reflectors they often constitute the first shield layer.

3.24 Particle Reactions. Examples of these are the (n, α) reactions in B^{10} and Li^6 and the (n, p) reaction in N^{14} . When a charged particle such as a proton or an α particle is released, there either is no accompanying γ ray or only one of low energy. For the cases of particle reactions in lithium and nitrogen, there are no γ rays, and for the case of B^{10} , there is one 0.493-Mev γ ray which is produced in 93 per cent of the particle reactions induced by thermal neutrons. This fact legislates in favor of adding B^{10} , N^{14} , or Li^6 to a biological shield. B^{10} and Li^6 are particularly desirable because of the fact that they exhibit large cross sections for these particle reactions. They can thus be thought of as strong capture γ -ray suppressors. Table 10 gives pertinent data on these nuclei. It is to be noted that there is also a cross section of

.08 barn for pure capture (n, γ) in N^{14} , and in this case 10.8 Mev of capture γ rays are given off.

3.25 Effect of Neutron Energy. Because of the fact that there are essentially no capture processes occurring at high energy, the attenuation of the most penetrating neutrons in a biological shield is accomplished largely by one inelastic followed by many elastic collisions. The total cross section of most materials decreases with increasing neutron energy, this effect being stronger in some elements than others, notable examples being hydrogen and lead, which have significantly greater cross sections at 2 than at 8 Mev. Because of this general trend in cross sections, the neutrons travel farthest on their first flight, on the average. Following each collision they are of lower energy and consequently travel shorter and shorter distances between collisions as they are slowed down within the shield. This effect is especially pronounced in shields which are highly hydrogenous. In dry shields, such as ordinary

Table 11. Dominant Energy in Hydrogenous Shields with U^{235} Fission Spectrum

t_{H_2O} , cm	$E_{Dom}^{(1)}$, Mev	$E_{Dom}^{(2)}$, Mev	$N_H t$, cm ⁻²	$E_{Dom}^{(1)}$, Mev
10	2.1	...	50	1.8
20	3.3	...	100	2.7
30	4.2	4.5	200	4.2
40	4.9	...	300	5.3
50	5.6	...	400	6.2
60	6.2	6.3	500	7.0
70	6.8	...	600	7.7
80	7.3	6.6	700	8.4
90	7.8	...	800	9.1
100	8.2	...	900	9.7
120	9.0	8.0	1,000	10.2
140	9.9	...	1,200	11.2
160	10.6	...	1,400	12.2
180	11.3	...	1,600	13.1
200	12.0	...	1,800	14.0

t_{H_2O} = thickness of water at N. T. P. in shield, cm

N_H = density of hydrogen atoms, cm⁻³, $\times 10^{-22}$, in shield, average

= 6.7 for H_2O so that, e.g., $t_{H_2O} = 100$ cm corresponds to $N_H t = 670$ cm⁻²

t = shield thickness, cm

$E_{Dom}^{(1)}$ = dominant energy, Mev, calculated on basis of first collision in hydrogen

$E_{Dom}^{(2)}$ = dominant energy, Mev, based on calculations for water attenuation by Aronson, Certaine, and Goldstein, NDA-15C-60, 1954, reflecting effect of variations in oxygen cross section as well

concrete, the high-energy neutrons do not predominate so strongly but the trend is qualitatively the same. The result of the trend to lower cross sections at higher neutron energies is that those neutrons which escape the shield are dominantly those which were born at relatively high energies. For water shields, for example, in common thicknesses, the neutrons which penetrate the shield were born* in the region of 8 Mev. In concrete shields the dominant energy is about 8 Mev.† This most important energy, or *dominant energy*, as we shall call it, is determined by the interplay of the two factors of increasing penetrability with increasing neutron energy on the one hand and the decreasing population in the fission spectrum on the other hand. The dominant energy in a hydrogenous shield is given as a function of shield thickness in Table 11.

It will be noted that below about 1 Mev there is little or no inelastic scattering. Furthermore, elastic scattering on heavy nuclei gives only a small energy reduction per collision. As a consequence, a neutron shield made entirely of heavy elements would be unsatisfactory. The neutrons would be reduced to energies of the order of 1 Mev by inelastic scattering and subsequently would suffer many elastic scatter-

* This does not imply that the spectrum of effluent neutrons at the shield outer surface is peaked at this energy. These high-energy neutrons are moderated in the outer shield layers and escape mostly at much lower energies.

† For concrete shields less than 100 cm thick the dominant energy is about 2.5 Mev.

ings. In doing so they would be reduced only slowly in energy and diffuse through the shield. Another reason for abnormally high penetration of these shields is that many heavy elements exhibit resonances in their neutron cross section with corresponding regions of low total cross section. Neutrons in these energy regions find it easy to penetrate the shield. A particular example of this effect is noticed in the case of iron, which has a minimum cross section of only about 0.5 barn for neutrons of 26-keV energy. A shield of pure iron would be ineffective against neutrons for this reason. This effect is so serious that it is not permissible to have long pieces of a single element penetrating through the shield in the direction of outward travel. It is to be noted, however, that alloys consisting of several elements seldom exhibit minima in their total cross sections because the minima for the individual elements seldom occur in the same energy region. Nevertheless, it is essential that each biological shield contain a large amount of moderating material, hydrogen being preferred, to ensure that the neutrons do not diffuse at intermediate energies through the shield. The criterion for ensuring that sufficient moderator is present is that one sixth of the mean squared slowing-down distance shall be less than the square of the mean free path for high-energy neutrons; i.e.,

$$\frac{1}{6}\overline{r^2} < \lambda^2 \quad (11)$$

3.3 Effective Removal Cross Sections

Of the foregoing attenuation processes only two are significant for high-energy neutrons, these being elastic and inelastic scattering. It is possible to predict the performance of a biological shield, subject to the limitations of the previous paragraph, in terms of a linear combination of these two cross sections. In general, the entire inelastic scattering cross section and about one-half of the elastic scattering cross section are considered effective. This sum is a fair approximation to the effective removal cross section of the shielding material. It has been demonstrated that the attenuation of fission neutrons through most shields can be expressed by a simple exponential, using this *effective removal cross section*. Of course, the dominant energy, at which the elastic and inelastic scattering cross sections are taken for determination of the effective removal cross section, will vary from shield to shield depending on the composition and the thickness.

For hydrogenous shields the dominant energy can be seen from Table 11 to vary strongly with shield thickness, this being a consequence of the strong variation of hydrogen cross section with energy. A good approximation of the hydrogen cross section for the region from 1 to 12 Mev is

$$\sigma_H = \frac{10.97}{E + 1.66} \quad \text{barns} \quad (12)$$

where E is the neutron energy in million electron volts. Table 11 was computed using this cross section and Watt's fission spectrum, obtaining the maximum in the product of free-flight penetration times population in the fission source. More exact calculations by Aronson, Certain, and Goldstein¹⁴ show less hardening of the neutron spectrum in a water shield, as is seen by their values reported in the table.

For thick ($\lesssim 100$ cm of H_2O or equivalent) hydrogenous shields many removal cross sections have been measured. These are given in Table 12. It is to be noted that these cross sections are strictly applicable only when the extraneous material precedes the hydrogenous material. It is acceptable, however, to use them for other cases as well, provided a pure heavy component, such as a slab of iron or lead, does not constitute the outermost layer. In the latter case, the slab cannot be counted on for appreciable attenuation (a relaxation length of about 35 cm is generally used).

For nonhydrogenous shields, such as most of the concretes, it is necessary to determine the dominant energy in the same way, that is, by the maximum in the product of penetration and population in the fission spectrum. This is a long and difficult task, and since the attenuation is not a very strong function of the dominant energy, about 8 Mev is generally used if the thickness is 100 cm or more, 3 Mev if less.

Table 12. Effective Removal Cross Sections for Fission Neutrons*

Material	Cross section, barns/atom	Material	Cross section, barns/molecule
Aluminum.....	1.31	C ₇ F ₁₆	26.3
Boron.....	0.97	C ₂ F ₂ Cl	6.6
Beryllium.....	1.07	CH ₂	2.8
Bismuth.....	3.49	B ₄ C	4.3
Carbon.....	0.81	D ₂ O	2.8
Chlorine.....	1.2		
Copper.....	2.04		
Fluorine.....	1.29		
Iron.....	1.98		
Lithium.....	1.01		
Nickel.....	1.89		
Oxygen.....	0.99		
Lead.....	3.5		
Tungsten.....	2.5		

* G. T. Chapman and C. L. Storrs, ORNL-1843, Aug. 31, 1955.

3.4 Dose Rate from Point Isotropic Fission Source

The process of calculating the attenuation of a point isotropic fission source in an infinite medium is as follows:

3.41 Hydrogenous Nonaqueous Shields. For hydrogenous shields (other than aqueous shields) of thickness t cm, the biological dose D at a distance R cm from unit source is

$$D(R,t) = \frac{4\pi r^2 D_H(r)}{4\pi R^2} e^{-\Sigma_r t} \quad \text{mrem/hr} \quad (13)$$

where $r = \rho_H t_H / 0.111$, cm

$\rho_H t_H$ = density of hydrogen, g/cm³, in hydrogenous shield multiplied by the thickness of hydrogenous shield, cm. If there are several layers of different hydrogen concentration, then $\rho_H t_H$ is the sum of these products for the several layers

$4\pi r^2 D_H(r)$ = dose, mrem/hr, in a pure hydrogen shield of thickness r cm, multiplied by $4\pi r^2$ (obtained from curve a of Fig. 5), source strength 1 neutron/sec

$\Sigma_r t$ = macroscopic removal cross section, cm⁻¹, for all elements in the shield other than hydrogen, multiplied by the shield thickness, cm. If there are several layers of different composition, then $\Sigma_r t$ is the sum of these products for the several layers. Some microscopic removal cross sections are given in Table 12, and Σ_r / ρ , the quotient of macroscopic cross section and density, is given as a function of atomic number in Fig. 6

3.42 Aqueous Shields. For hydrogenous shields in which the hydrogenous material is water, the biological dose is

$$D(R,t) = \frac{4\pi r^2 D_{H_2O}(r)}{4\pi R^2} e^{-\Sigma_r t} \quad \text{mrem/hr} \quad (14)$$

where $4\pi r^2 D_{H_2O}(r)$ = dose, mrem/hr, in a pure water shield multiplied by $4\pi r^2$ (obtained from curve b of Fig. 5)*

$\Sigma_r t$ = macroscopic removal cross section, cm⁻¹, for all elements in the shield other than those in water, multiplied by the shield thickness, cm (use Table 12 or Fig. 6)

$\rho_{H_2O} t_{H_2O}$ = water density, g/cm³, multiplied by thickness of water portion of shield, cm

$$r = \frac{\rho_{H_2O} t_{H_2O} (\text{g/cm}^2)}{1 \text{ g/cm}^3}$$

* For thick water shields beyond the range of Fig. 5 the γ -ray dose predominates and governs thickness.

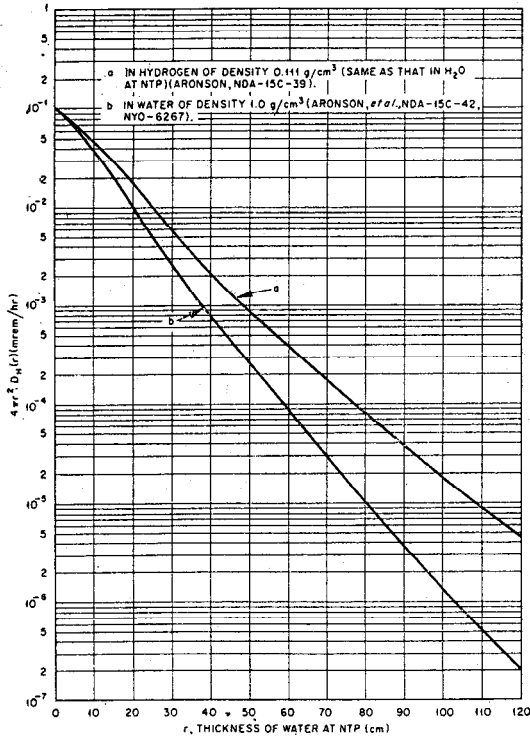


Fig. 5. Dose as a function of distance from a point isotropic fission source.

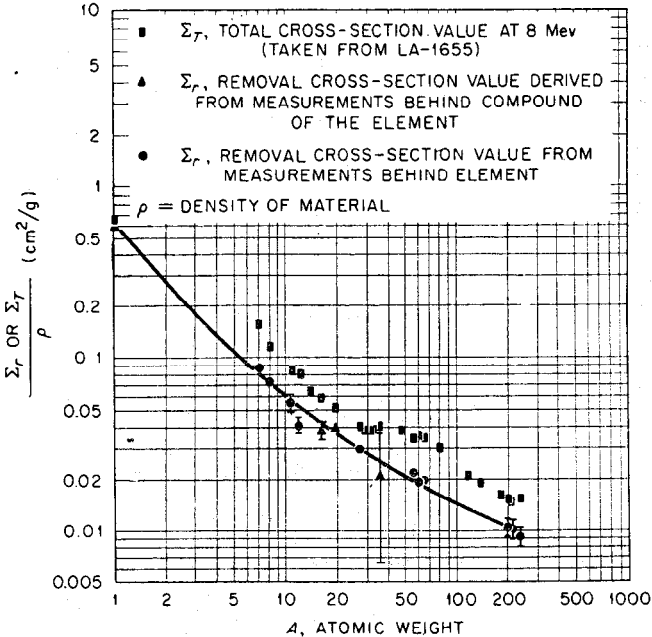


Fig. 6. Neutron shielding ability per unit weight of a material as a function of atomic weight.

3.43 Nonhydrogenous Shields. For nonhydrogenous shields, such as the concretes (hydrogen atomic per cent less than ~ 50), the dose is calculated by several steps. First the sum of the removal cross sections for the various materials in the shield is determined as a function of energy:

$$\Sigma_r(E) = f_1 \Sigma_1(E) + f_2 \Sigma_2(E) + f_3 \Sigma_3(E)$$

where $\Sigma_1(E)$ = macroscopic hydrogen cross section, cm^{-1}

$$f_1 \cong 1$$

$\Sigma_2(E)$ = macroscopic total cross section of oxygen plus carbon, cm^{-1}

$$f_2 = 0.5, E < 4 \text{ Mev (i.e., no inelastic scattering)}$$

$$f_2 = 0.75, E > 4 \text{ Mev}$$

$\Sigma_3(E)$ = macroscopic total cross section of all other elements in the shield, cm^{-1}

$$f_3 \cong 0.75 \text{ (i.e., all of the inelastic scattering and half of the elastic scattering cross sections are effective)}$$

If the elastic and inelastic cross sections Σ_{el} and Σ_{in} are known, however, it is better to compute the removal cross section of the shield as follows:

$$\Sigma_r(E) = f_1 \Sigma_1(E) + \frac{1}{2} \Sigma_{el}(E) + \Sigma_{in}(E)$$

The maximum of the function

$$Q(E) = N(E) e^{-\Sigma_r(E)t}$$

is then computed where t is a first estimate of the shield thickness. The value of E for which $Q(E)$ is a maximum [$dQ(E)/dE = 0$] is the dominant energy E_0 Mev. For

Table 13. Biological Effect of Neutrons*

Neutron energy, Mev	Flux, neutrons/(cm^2)(sec), to give laboratory tolerance = 7.5 mrem/hr (assuming 40 hr/week)	(Mrem/hr) / [(neutrons)/(cm^2)(sec)]
2.5×10^{-8} (thermal)	2,000	3.75×10^{-3}
10^{-4}	1,550	4.8×10^{-3}
4×10^{-3}	1,700	4.4×10^{-3}
2×10^{-2}	830	9.0×10^{-3}
0.1	250	3×10^{-2}
0.5	90	8.3×10^{-2}
1.0	60	1.25×10^{-1}
2.5	60	1.25×10^{-1}
5.0	55	1.36×10^{-1}
7.5	50	1.5×10^{-1}
10.0	50	1.5×10^{-1}

* From data of W. S. Snyder, Oak Ridge National Laboratory, submitted to Subcommittee on Neutrons of National Committee on Radiological Protection, 1956.

most concretes computation of the maximum is difficult, and a value of 8 Mev can be used for E_0 .

The biological dose is then given by

$$D_B(R,t) = \frac{Sb(E_0)}{4\pi R^2} e^{-\Sigma_r(E_0)T} \text{ mrem/hr} \quad (15)$$

where S = source strength, neutrons/sec (regardless of energy—for conservatism—in the fission source)

$b(E_0)$ = biological effect of unit flux of neutrons of energy E_0 , (mrem/hr)/[neutrons/(cm^2)(sec)] (given in Table 13)

A better estimate of the biological dose can be had by integrating over all source energies, thus:

$$D_B(R,t) = \frac{S}{4\pi R^2} \int_{E=0}^{\infty} N(E) e^{-\Sigma_r(E)T} b(E) dE \quad (16)$$

Because the integrand is not analytic, the integration must be done by hand, but since for energies above about 5 Mev both $b(E)$ and $\Sigma_r(E)$ are nearly constant, at least this part of the integration can be done easily, making use of the integrated fission spectrum in Table 15.

3.44 Shielding of Delayed Neutrons. As is evident from Table 16, the delayed neutrons are of energies below the threshold for inelastic scattering for many elements. As a consequence it is highly desirable to shield delayed neutrons with hydrogenous materials, for which the cross sections are large and the energy degradation per collision high. However, the cross section of hydrogen below 1 Mev does not increase

Table 14. Attenuation by Water of 2.0*- and 0.9†-Mev Neutrons, Unit Point Source (Neutrons/Sec), Detector a Distance R Cm away
(RBE = 10)

R , cm	Dose, mrem/hr, 0.9-Mev source	Dose, mrem/hr, 2.0-Mev source
10	2.7×10^{-6}	3.7×10^{-5}
20	1.3×10^{-7}	1.5×10^{-6}
30	4.8×10^{-9}	8.1×10^{-8}
40	4.5×10^{-9}
50	3.5×10^{-10}
60	2.2×10^{-11}

* R. Aronson, J. Certaine, and H. Goldstein, NDA 15C-60 (NYO-6269), 1954.

† T. Rockwell III (ed.), "Reactor Shield Design Manual," TID-7004, 1956; see also K. Shure and P. A. Roys, Report WAPD-T-226, August, 1955.

(fractionally) with decreasing energy as much as it does for energies above that energy, with the result that for low energies the build-up factors in hydrogenous shields are quite high. Attenuation data for 2.0- and 0.9-Mev sources in water are given in Table 14. These can be corrected safely for other shielding materials on the basis of hydrogen content alone. Of course, the delayed neutrons have lower energies, so that it is conservative to use the values in the table for estimating doses.

3.5 Heating in Shields by Neutrons

Neutrons cause heating in shields by each of four processes. In the first place, in elastic collisions they cause nuclei to recoil, and these recoiling nuclei deposit their kinetic energy as heat in the shield. In inelastic scattering, the nuclei which have been excited give off γ rays as well as depositing some kinetic energy, and both of these components heat the shields. Of these, in general, the kinetic energy can be ignored. Neutrons are captured in shields, and the capture γ rays cause heating in the shield. The fourth process by which neutrons cause heating in shields is by charged particle reactions, such as (n, α) and (n, p) as described previously. In general, the important aspect of heating in shields is the thermal stresses which are induced thereby. Therefore, any calculational method which tends to overemphasize the average gradient in the heating distribution will be a conservative calculation. The exact calculation of heating in a shield is a very complicated problem and will, in general, require solution by a high-speed computing machine, perhaps utilizing the Monte Carlo method. Some approximations by hand computation, however, may be desirable. Estimates of the neutron heating will be possible by the method to be outlined in the following paragraphs.

Heating by elastic scattering can be estimated to be accomplished on the first elastic scattering collision. This will be conservative if the heat is removed from the outside (far from the source). For hydrogen, on the average, one-half of the energy is given to the recoiling proton in an elastic collision. However, the neutron will suffer subsequently another collision at some distance not far removed from the first and give up again one-half of its remaining energy on the average. Thus the heat

deposition due to elastic collisions in hydrogen is at least as far from the core (or source) as would be calculated on the basis that the total neutron energy is released on the first elastic collision. The calculation for this deposition then is a simple exponential, using the total hydrogen cross section.

If the heat removal is from the inside instead, it is conservative to assume that the energy is deposited at some distance beyond the first collision. This distance can be taken to be the "displacement distance" τ/λ where τ is the Fermi age to thermal energy and λ is the relaxation length of the uncollided flux.*

W. S. Snyder gives curves of physical and biological dose as a function of distance into a 30-cm-thick slab of tissue (see Figs. 5 to 13 of Sec. 7-2). Since the physical dose is primarily attributable to recoil protons, it is permissible to use the dose curves to predict heating in hydrogenous media. Of course, at neutron energies appreciably below about 1 Mev, the recoil protons do not override in importance those from the $N^{14}(n,p)C^{14}$ reaction, so that the biological curves do not properly predict heating except in tissue. Thus, the heating at a depth x in a hydrogenous medium is given in terms of the physical dose in tissue as follows:

$$H(E,x) \cong 10^{-5} \frac{N_H}{N_H'} D_F(E,x') \quad (\text{watts})(g)/(\text{neutrons})(\text{cm}^2)(\text{sec}) \quad (17)$$

where N_H = hydrogen density, atoms/cm³ $\times 10^{-22}$, for material in which heating is to be calculated

$$N_H' = \text{hydrogen density in tissue} \times 10^{-22} \\ = 5.98$$

$$x' = (N_H/N_H')x, \text{ cm}$$

$D_F(E,x')$ = physical dose, rads/(neutron)(cm²), from Snyder's curves (Figs. 5 to 13 of Sec. 7-2).

Two other interesting facts, from a heating-in-shields point of view, are to be seen in Snyder's curves. The energy deposited by recoils of heavier nuclei such as oxygen, carbon, and nitrogen accounts for less than 10 per cent of that from all recoils. The heating from capture γ rays is given also, and it is seen to be dominant at the greater depths, owing, of course, to the greater penetration of γ rays in tissue.

For oxygen and carbon in the absence of hydrogen many collisions are required to reduce the neutron energy, so that age calculations, multigroup calculations, or Monte Carlo calculations are required. For all other nuclei, the fast neutron collisions probably result about equally in inelastic scattering and elastic scattering. Since in the elastic scattering only a small fraction of the energy is given to the recoiling nucleus, this will represent a negligible fraction of the total heating due to neutrons. The inelastic scattering γ rays will dominate strongly.

In conclusion, it may be said that if the shield contains either hydrogen or a significant quantity of heavy element, then these two components will do the large part of energy absorption. The ratio of inelastic scatterings in the heavy elements and elastic scattering in hydrogen will depend, of course, on the relative cross sections for these two processes in the shield material. In case the shield is largely made up of other elements such as oxygen and carbon, then the energy will be transferred by elastic collisions in either of these light elements. The calculation of energy deposition in this case is most properly carried out by the methods described in neutron moderation in the reactor physics section of this handbook. A rough approximation of the heat deposition can, of course, be had even in this case, using exponential attenuation with the effective removal cross section.

As an example of the calculation of the heat deposition in a shield, the following situation will be studied: A point source of fission neutrons will be presumed to be surrounded by a shield of barytes concrete. The problem will be to calculate the heat distribution due to the incidence of the neutrons on the barytes.

The composition of barytes concrete is given in Table 22 in Art. 6 on Shield Materials. The source will be assumed to be at the center of a spherical hole of radius a in the concrete. Examination of the concrete materials reveals that energy may be

* See, for example, Ref. 15, pt. 2, pp. 100ff.

expected to be deposited largely by two processes: elastic scattering in hydrogen and inelastic scattering in Ba, Fe, Ca, and Si. Other processes, such as elastic scattering in oxygen, may contribute to the attenuation, largely because of neutron deflection, but will not reduce neutron energy by a large fraction. Therefore, the ratio of elastic scattering in hydrogen to inelastic scatterings in heavy elements will be the ratio of the two macroscopic cross sections.

The neutron heating (excluding secondary γ heating) is given by

$$H_n(R) = \frac{S}{4\pi R^2} \int_0^\infty N(E) \frac{\Sigma_1 \Sigma_r}{\Sigma_1 + \Sigma_3} E \exp[-(R-a)\Sigma_r] dE \quad \text{Mev}/(\text{cm}^3)(\text{sec}) \quad (18)$$

where S = source strength, neutrons/sec

R = distance from source to measuring point, cm

a = radius of hole containing source, cm

$N(E)$ = distribution function for neutron energy in source, normalized so that $\int N(E) dE = 1$

$\Sigma_r(E)$ = removal cross section of barytes concrete for neutrons of energy E Mev, cm^{-1}

$$= \Sigma_1(E) + f_2 \Sigma_2(E) + f_3 \Sigma_3(E)$$

$\Sigma_1(E)$ = macroscopic hydrogen total cross section as it appears in barytes concrete, cm^{-1}

$\Sigma_2(E)$ = macroscopic total cross section of oxygen as it appears in barytes concrete for neutrons of energy E Mev, cm^{-1}

$f_2(E)$ = effectiveness factor for oxygen to obtain removal from total cross sections: $f_2 \approx 1/2$ for $E < 4$ Mev; $f_2 = 3/4$ for $E > 4$ Mev

$\Sigma_3(E)$ = macroscopic total cross section of inelastic scatterers, Ba, Fe, Ca, Si, as they appear in the concrete for neutrons of energy E Mev, cm^{-1}

$f_3(E)$ = effectiveness factor to obtain removal from total cross section for inelastic scatterers: $f_3 \approx 3/4$ for $E > 1$ Mev; $f_3 \approx 1/2$ for $E < 1$ Mev

While the integral above appears to be difficult to evaluate, actually relatively few energy intervals will be needed, since the largest contribution to the heating will be for the energy range of about $1/2$ to 5 Mev.

The sources of inelastic scattering can be calculated by an integral much like that of Eq. (18) except that in place of Σ_1 in the numerator, Σ_{in} , the inelastic scattering cross section, is used. In the absence of exact data, $1/2 \Sigma_3$ can be used. The spectrum of inelastic scattering γ rays is known only for a few isotopes, so some assumption must be made. The simplest reasonable assumption is that the γ s have nearly all the neutron energy and that it comes off in a single photon. For high neutron energies ($E > 6$ Mev), the inelastic scattering γ rays may be expected to come off in several photons of lower energy if the capture γ s of that element do so. This is not a very reliable rule, however, as the emitting isotopes are different in the two cases.

The inelastic scattering γ rays will, of course, travel isotropically from their points of production before losing energy to the medium, and the calculation of this effect is one largely of geometry. The total result of this travel will be to alleviate the gradient in heat production. Again, if cooling is from the outside, it is conservative to ignore this further travel in considerations of heat stress and to assume that the γ energy is deposited at the point of scatter.

The neutrons which are slowed down in the concrete are captured and give rise to capture γ rays. Because neutron capture takes place dominantly at or near thermal energies, the neutrons for this case are calculated according to the age diffusion picture, and these calculational methods are described in the reactor physics section of this handbook. Similarly, the deposition of heat due to particle reaction in the shield is again an effect proportional to thermal neutron flux and can be calculated according to standard neutron diffusion techniques.

Very often it is necessary to calculate the heating due to capture γ rays produced within a slab of material, such as a steel thermal shield or pressure shell. Enlund¹⁶ has treated this problem, using exponential distribution of the neutrons being captured. For the γ -ray attenuation he used an expression derived by H. Goldstein¹⁷

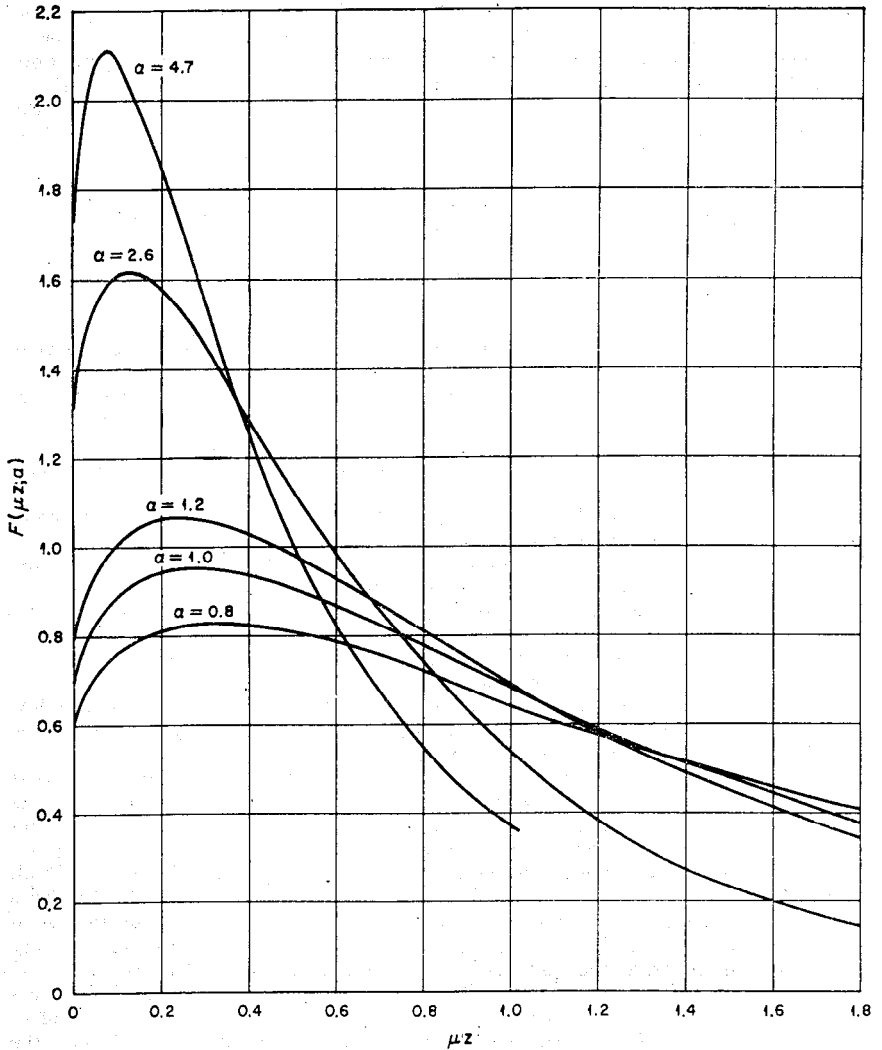


FIG. 7. Energy absorption from capture γ rays: the function $F(\mu z, \alpha)$.

on the basis of conservation of energy. Thus the heating at R cm due to a point source of unit strength (one photon per second) of photons of energy E Mev in an infinite medium is

$$H(R) = E\mu_a \left(1 + \frac{\mu - \mu_a}{\mu_a} \mu R \right) \frac{e^{-\mu R}}{4\pi R^2} \quad \text{Mev}/(\text{cm}^2)(\text{sec}) \quad (19)$$

where μ and μ_a are described in Art. 1.

The problem Enlund has solved is for an infinite plane source of neutrons emitting a current I_0 neutrons/ $(\text{cm}^2)(\text{sec})$ into an infinite plane slab with source on one side, giving a flux within the slab described by

$$\phi(x) = \frac{I_0 e^{-Kx}}{KD}$$

where $I_0 =$ neutron current, $\text{cm}^{-2} \text{sec}^{-1}$

$$= -D \frac{d\phi}{dz} \text{ at } z = 0$$

$$K = \sqrt{3\Sigma_a\Sigma_t}, \text{ cm}^{-1}$$

$\Sigma_a =$ macroscopic absorption cross section, cm^{-1}

$\Sigma_t =$ macroscopic transport cross section, cm^{-1}

$D =$ diffusion coefficient, cm

$z =$ coordinate of distance into slab from source, cm

$$\Sigma_a\phi(z) = KI_0e^{-Kz}$$

$=$ density of absorptions at z , $\text{cm}^{-3} \text{sec}^{-1}$

$N(E) =$ fraction of neutron captures which give a photon of energy E Mev

$\mu_a(E) =$ energy absorption coefficient, cm^{-1} , for γ rays

$\mu(E) =$ linear attenuation coefficient, cm^{-1}

$$\alpha = K/\mu$$

The heating at z due to γ rays of energy E is $H(z,E)$. Total heating is obtained by summing over-all capture γ rays:

$$H(z,E) = 8.0 \times 10^{-14} N(E) E I_0 \mu_a(E) \left[F(\mu z, \alpha) + \alpha \frac{\mu - \mu_a}{\mu_a} k(\mu z, \alpha) \right] \text{ watts/cm}^3 \tag{20}$$

where

$$F(\mu z, \alpha) = e^{-\alpha\mu z} \left\{ \alpha\mu z [-Ei(-\mu z)] + \overline{Ei}[\mu z(\alpha - 1)] + \ln \frac{\alpha + 1}{\alpha - 1} \right\} \text{ for } \alpha > 1$$

$$F(\mu z, \alpha) = e^{-\mu z} \{ e^{\mu z} [-Ei(-\mu z)] + \ln \mu z + \ln(2\gamma) \} \text{ for } \alpha = 1$$

$$\ln \gamma = 0.5772$$

$$F(\mu z, \alpha) = e^{-\alpha\mu z} \left\{ e^{\alpha\mu z} [-Ei(-\mu z)] + Ei[-\mu z(1 - \alpha)] + \ln \frac{1 + \alpha}{1 - \alpha} \right\} \text{ for } \alpha < 1$$

$$k(\mu z, \alpha) = \frac{e^{-\alpha\mu z}}{\alpha - 1} \left[e^{\mu z(\alpha - 1)} - \frac{2}{(\alpha + 1)} \right]$$

Values of $F(\mu z, \alpha)$ are given in Fig. 7 and values of $K(\mu z, \alpha)$ are given in Fig. 8. For the functions $-Ei(-x)$ and $\overline{Ei}(x)$ see Table 15 of Sec. 1-2.

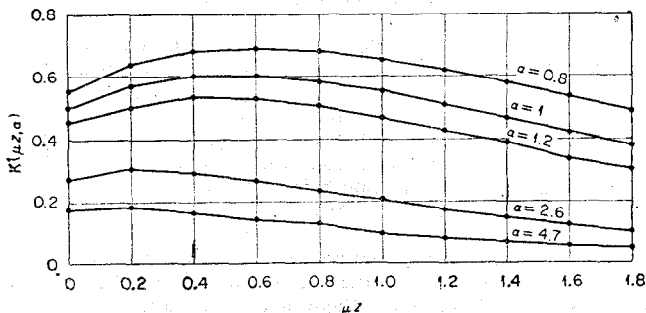


Fig. 8. Energy absorption from capture γ rays: the function $K(\mu z, \alpha)$.

3.6 Secondary γ Rays—Biological Effects

As has already been mentioned, reactor shields become sources of γ rays owing to capture and inelastic scattering of neutrons. These sources of γ rays constitute a biological hazard which must be taken account of in calculating shield effectiveness. The first requirement is to determine the distribution of capture and inelastic scattering γ rays in the medium. The distribution of inelastic scattering γ rays has already been described in the discussion on heating in the shield. The distribution of capture γ rays, on the other hand, will vary somewhat from that for the inelastic scattering

because of the age displacement between the first collision of the neutrons and their actual capture after slowing down. In general, the rate of removal of neutrons from the penetrating beam is equal simply to the derivative of the neutron flux at any point in the shield. That is to say, it is equal to the macroscopic removal cross section multiplied by the neutron flux as calculated by the methods described in the foregoing paragraphs; i.e.,

$$R = - \frac{dI(z)}{dz} \cong \frac{I(z)}{\lambda} \quad (21)$$

where R = rate of removal of fast neutrons

I = current of fast neutrons

λ = relaxation length, cm, or inverse of macroscopic removal cross section, average

These removed neutrons can be presumed to slow down according to a Gaussian distribution. Convolution* of this distribution with an assumed exponential attenuation of fast neutrons gives the total arrivals at thermal energies as a function of position. Ignoring diffusion at thermal energies, the rate of arrivals at thermal energy is equal to the rate of absorption, i.e., $\Sigma_{a,th} \phi_{th}(z)$. The result is

$$\begin{aligned} \Sigma_{a,th} \phi_{th}(z) &= \frac{I(z)}{\sqrt{\pi\lambda}} e^{\tau/\lambda z} \int_{x=\frac{\sqrt{\tau}}{\lambda} - \frac{z}{\sqrt{4\tau}}}^{\infty} e^{-x^2} dx \\ &= \frac{I(z)}{2\lambda} e^{\tau/\lambda z} [1 + E(m)] \end{aligned} \quad (22)$$

$$\text{where } E(m) = \frac{2}{\sqrt{\pi}} \int_0^m e^{-x^2} dx$$

τ = Fermi age to thermal of dominant energy, cm^2

$m = (z/4\tau) - (\sqrt{\tau}/\lambda)$

The term $E(m)$ is given as the "error integral" in Table 17 of Sec. 1-2. For $m = 1$, $E(m) = 0.84$, so for thick shields it is sufficient to use the value 2 for the quantity in the brackets.

The next step in dealing with secondary γ rays is to determine the relative attenuation of the shield for neutrons and γ rays. If the shield has a longer relaxation length for γ rays than for neutrons, then the γ rays which are produced in the first couple of mean free paths of the shield will constitute the important source of γ rays in so far as secondary γ rays are concerned. One can therefore take the source of γ rays as those produced within two mean free paths of the inner surface. Presume that these are produced as predicted above, or approximately at a distance equal to τ/λ from the inner surface, and attenuate them through the shield by the standard methods described in the γ -ray section. If, on the other hand, the neutrons penetrate the shield more easily than the γ rays, then because of the greater biological importance of the neutrons no account need be taken of the secondary γ rays produced by the neutrons in the shield, the neutrons themselves constituting the only significant source of radiation. This does not say that the γ rays produced in the core and the reflector may not be important. In general, the biological shield thickness is determined by the most penetrating component of radiation.

4 NEUTRON SOURCES

The fission products emit neutrons which are classed as "prompt" if the time between fission and emission is not measurable or "delayed" if it is measurable. These fission neutrons are discussed below, along with the production of neutrons from artificial sources.

* Integration of the product over all space.

4.1 Prompt Fission Neutrons

The neutrons emitted at the time of fission of U^{235} from its fission fragments are distributed in energy from 0.075 Mev¹⁸ (or lower) to about 17 Mev.¹⁹⁻²¹ The distribution of these "prompt" neutrons is quite closely described by the approximate formula of Watt,²⁰

$$N(E) dE = 0.484 \sinh \sqrt{2E} e^{-E} dE \quad (23)$$

where $N(E) dE$ = number of neutrons of energy E to $E + dE$ per fission neutron emitted

E = neutron energy, Mev

Values of $N(E) dE$ are given in Table 15. A simpler approximate expression that is

Table 15. The U^{235} Fission Spectrum of Prompt Neutrons*

[$N(E) dE$ is the fraction of neutrons of energy E to $E + dE$ from thermal-neutron fission of U^{235}]

E , Mev	$N(E)$, Mev ⁻¹	$\int_0^E N(E) dE$	$\int_E^\infty N(E) dE$
0.1	0.2023	0.014	0.9860
0.2	0.2676	0.377	0.9623
0.3	0.3068	0.663	0.9337
0.4	0.3300	0.987	0.9013
0.5	0.3450	0.1321	0.8679
0.6	0.3528	0.1669	0.8331
0.7	0.3557	0.2027	0.7973
0.8	0.3542	0.2385	0.7615
0.9	0.3513	0.2729	0.7271
1.0	0.3446	0.3082	0.6918
1.1	0.3368	0.3425	0.6575
1.2	0.3271	0.3759	0.6241
1.3	0.3179	0.4074	0.5926
1.4	0.3073	0.4383	0.5617
1.6	0.2841	0.4983	0.5017
1.8	0.2604	0.5631	0.4369
2.0	0.2371	0.6028	0.3972
2.5	0.1839	0.7073	0.2927
3.0	0.1384	0.7876	0.2124
3.5	0.1026	0.8476	0.1524
4.0	0.07472	0.8914	0.1086
4.5	0.05381	0.9192	0.0808
5.0	0.03847	0.9463	0.0537
5.5	0.02729	0.9624	0.0376
6.0	0.01916	0.9739	0.0261
6.5	0.01336	0.9821	0.0179
7.0	9.316×10^{-3}	0.9876	0.0124
7.5	6.436	0.9916	0.0084
8.0	4.423	0.9943	0.0057
8.5	3.034	0.9960	0.0040
9.0	2.076	0.9973	0.0027
9.5	1.418	0.9982	0.0018
10.0	9.53×10^{-4}	0.9988	1.211×10^{-3}
11.0	4.384	0.9994	5.501×10^{-4}
12.0	1.994	0.9998	2.473
13.0	8.953×10^{-5}	0.9999	1.103
14.0	3.997	1.0	4.875×10^{-5}
15.0	1.771	1.0	2.148

* Calculated from the formula of B. E. Watt, *Phys. Rev.*, **87**: 1037 (1952). From J. E. Evans, "Fast Neutron Spectra from the Water Boiler," LA-1395, AEC-D 3073, Los Alamos Scientific Laboratory, March, 1951.

good to 15 per cent from $E = 4$ to 12 Mev is

$$N(E) dE = 1.8e^{-0.75E} dE \quad (24)$$

The fission spectrum of Pu^{239} has also been measured²² and is fitted fairly well by Eq. (23), although there appears to be a somewhat greater abundance of higher

energy neutrons. The statistical accuracy is not adequate to certify a genuine difference, however.

4.2 Delayed Neutrons

Some of the fission products decay radioactively by neutron emission. These "delayed" neutrons are of lower energy than the prompt neutrons and are much less numerous²³ (Table 16).

Table 16. Delayed Neutrons*.²³

Half-life, sec	Mean energy, kev	Absolute yields of delayed neutrons per 10 ⁴ total neutrons emitted		
		U ²³⁵	U ²³³	Pu ²³⁹
55.07 ± 0.49	250 ± 20	2.11	2.24	0.73
21.13 ± 0.33	460 ± 10	14.1	7.76	6.32
5.56 ± 0.14	405 ± 20	12.6	6.54	4.48
2.26 ± 0.08	450 ± 20	25.4	7.24	6.91
0.611 ± 0.074		7.40	1.34	1.81
0.244 ± 0.020		2.68	0.87	0.94
		Total 64.3	26.0	21.2

* Half-lives and yields from LA-2118, G. R. Keepin, T. F. Wimett, R. K. Ziegler, "Delayed Neutrons from Fissionable Isotopes of Uranium, Plutonium, and Thorium," p. 32 (February, 1957), using $\nu = 2.46, 2.54, \text{ and } 2.88$ for U²³⁵, U²³³, and Pu²³⁹ respectively, and taking mean values for the six half-lives. Mean energies from R. Batchelor and H. R. McK. Hyder, *Jour. Nuc. En.*, **3**: 7 (1956).

4.3 Artificial Sources

4.31 (α, n) Sources. It is possible to produce neutrons from α -particle bombardment of certain nuclei. The α particles can come from radioactive nuclei, so that a small pill which includes an α emitter (e.g., radium) and a target material (e.g.,

Table 17. Alpha Neutron Sources*

α emitter	Target	Yield, neutrons/(sec)(curie of α s)
Po	Li	5×10^4
	Be	2.3×10^6
	B	6×10^6
Ra	Al	2×10^4
	Be	1.7×10^7
Pu ²³⁹	B	7×10^6
	Be	1.5×10^6

* See also Wilmot N. Hess, UCRL-3839, "Neutrons from (α, n) Sources," July, 1957.

Table 18. Photoneutron Sources

γ -ray emitter	Target nucleus	Neutron energy, kev	Half-life
Sb ¹²⁴	Be	30	60 days
Ga ⁷²	D ₂ O	135	14.35 hr
La ¹⁴⁰	D ₂ O	130	40 hr
	Be	730	40 hr
Y ⁸⁸	Be	160	105 days
Mn ⁵⁶	D ₂ O	210	2.59 hr
Na ²⁴	D ₂ O	260	15 hr
	Be	960	15 hr

boron) can be made which acts as a convenient neutron source. Data on some useful sources are given in Table 17.

4.32 Photoneutron Sources. It is also possible to produce neutrons by the interaction of γ rays on nuclei. Certain nuclei have sufficiently low thresholds in γ -ray energy for this process to enable the construction of convenient small photoneutron sources. The yield is small, but the neutrons are monoenergetic for each γ -ray energy. Data on these are given in Table 18.

5 GEOMETRY

In the previous articles attenuation from point sources of γ rays or neutrons has been described. In practice, radioactive sources such as cesium-137, cobalt-60, or polonium-beryllium neutron sources can be thought of as point sources; however, reactor shielding problems deal with arrays of sources distributed throughout a volume of absorbing material. In order to determine the biological effects of arrays of sources, it is necessary to integrate over all the sources. The net resultant biological dose due to an array of sources is simply the sum of the effects of the individual sources. This section describes the processes of integration over arrays of sources. Transformations for surface sources in homogeneous shields with unspecified attenuation functions are first discussed, after which those with partially specified attenuation functions are described. Methods for determining the leakage flux from volume-distributed sources are then outlined, and methods of estimating build-up factors for dose from distributions are given. Finally, formulas to determine the flux in various source-shield geometries are listed.

5.1 Transformations for Surface Sources in Homogeneous Shields with Unspecified Attenuation Functions

The response of a detector to a nearby point source can be described in terms of an attenuation kernel, which in general is a function of the type of source, the type of detector (or receptor), the type of material interposed between the two, and the separation distance between source and detector. The source can for the moment be any source of unit strength. It is presumed that the detector records biological dose and has no directional dependence. *The medium is presumed to be uniform throughout with no preferred direction for attenuation.* In this situation the dose due to a point source of strength S at a distance R from the detector can be described as

$$D_{pt}(R) = SG(R) \quad (25)$$

In this equation the function $G(R)$ is the attenuation kernel. It is, in fact, the subject of Arts. 1 and 3.

5.11 Point to Plane Source. If the attenuation kernel $G(R)$ is known for all values of R , it is possible to obtain the dose from a surface distribution of sources in a homogeneous medium by integration:

$$D = \int_{\text{surface}} sG(R) dA \quad (26)$$

where s = source strength per unit area

dA = element of area on source plane

R = distance from area element to detector

When $G(R)$ is known either from measurement with a point source or from calculations (such as were described in Arts. 1 and 3), the following equation is useful:

$$D_{p1}(z, \infty) = 2\pi s \int_z^{\infty} G(R)R dR \quad (26a)$$

where $D_{p1}(z, \infty)$ is the dose at distance z from an infinite plane source.

5.12 Plane to Point Source. If the information which is known is the dose from a large plane distribution of sources, then it is convenient to differentiate Eq. (26a) to

obtain the kernel:

$$G(R) = -\frac{1}{2\pi s} \left[\frac{1}{z} \frac{d}{dz} D_{p1}(z, \infty) \right]_{z=R} \quad (27)*$$

5.13 Point to Plane Disk Source. In case the plane isotropic source of surface strength s is limited to a disk of radius a (Fig. 9), then the dose at a point on the axis a distance z from the disk is given by

$$D_{p1}(z, a) = 2\pi s \int_z^{\sqrt{z^2+a^2}} G(R) R dR \quad (28)$$

5.14 Plane Disk to Point Source. Unless the form of the attenuation kernel is known, the foregoing integral cannot be evaluated. However, the attenuation kernel can be obtained if the dose from the disk source is known everywhere on the disk axis.²⁴ Thus,

$$G(R) = -\frac{1}{2\pi s} \left[\frac{1}{z} \sum_{\nu=0}^{\infty} \frac{d}{dz} D_{p1}(\sqrt{z^2 + \nu a^2}, a) \right]_{z=R} \quad (29)*$$

Equation (29) is used to obtain the point-to-point kernel from data from a finite disk source (such as that at the Oak Ridge National Laboratory Lid Tank Shielding

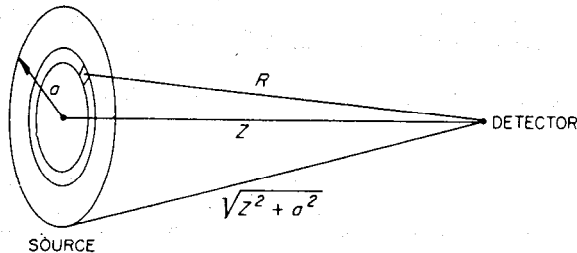


Fig. 9. Geometry for disk source and homogeneous shield.

Facility) in the following way: (1) For a given value of R , for which the kernel is required, calculate $\sqrt{R^2 + a^2}$, $\sqrt{R^2 + 2a^2}$, . . . , etc.; (2) from the experimental data, find the derivative of the dose at the abscissas R , $\sqrt{R^2 + a^2}$, $\sqrt{R^2 + 2a^2}$, . . . , i.e., for $\nu = 0, 1, 2$, etc.; (3) add these together to form the indicated sum, divide by $2\pi s R$, and the negative of the result is the dose to be expected at a distance R from a point source of unit strength.

For large enough source plates the foregoing sum converges rapidly and only one term [i.e., Eq. (27)], or at most a few terms, is required for accurate evaluation. For very small source plates and large distances the source can be considered to be a point source of strength As , A being the source area. Equation (25) then applies.

The derivative of the dose function can be characterized by a relaxation length, or "e-folding length," λ , which is defined for this dose function as

$$\lambda(z) = -\frac{D_{p1}(z, a)}{(d/dz)D_{p1}(z, a)} \quad (30)$$

If $\lambda(z)$ is only slowly varying in z , then an approximate form for Eq. (29) can be used which obviates the summation:

$$G(R) \cong \left[\left(\frac{1}{4\pi z s \lambda} + \frac{1}{\pi a^2 s} \right) D_{p1}(z, a) \right]_{z=R} \quad (31)*$$

* The quantities in the brackets are to be evaluated at $z = R$.

This should be used only if (1) λ is nearly a constant in the region $z \gtrsim R$ and (2) $a^2 < 4\lambda z$.

If condition 1 is not satisfied, Eq. (29) must be used. If condition 2 is not satisfied, Eq. (27) will give a good estimate of $G(R)$.

5.15 Finite Disk to Infinite Plane Source. It is possible to determine the dose to be expected from an infinite plane of sources in terms of the dose at all axial points due to sources spread evenly on a finite disk:*

$$D_{p1}(z, \infty) = \sum_{\nu=0}^{\infty} D_{p1}(\sqrt{z^2 + \nu a^2}, a) \quad (32)$$

(Note: In this equation it is assumed that surface source strengths for disk and infinite plane sources are the same. If they are not, a true equation can be had by dividing each dose by the corresponding source strength.) The use of this equation is similar to that of Eq. (29). The summation can be avoided by the use of the following approximate inequality:

$$1 + \alpha > \frac{D_{p1}(z, \infty)}{D_{p1}(z, a)} \gtrsim \frac{1}{2} + \alpha \quad (33)$$

where

$$\alpha = \frac{2\lambda^2}{a^2} \left(\frac{z}{\lambda} + 1 \right)$$

and λ is defined by Eq. (30). For the approximate equality in Eq. (33) to be valid,

1. $\lambda(z)$ must be nearly constant in the region of use.
2. $a^2 < 4\lambda z + 4\lambda^2$.

If condition 1 is not satisfied, Eq. (32) must be used. If condition 2 is not satisfied, the dose on the disk axis will be nearly equal to that at corresponding distances from an infinite plane.

5.16 Plane to Spherical Shell Source. If an isotropic source of a given strength per unit area is spread on a spherical surface which is wholly within an attenuating medium, it is possible to predict the dose as a function of distance from this surface in terms of the dose from an infinite plane isotropic source of the same strength per unit area. The material inside the sphere must be the same in attenuation as that outside the source, and the source itself must be thin enough so that it does not affect the attenuation. This transformation can be used for the case of spherical or near-spherical reactors in which the spherical shell source will be an element of the volume source. The dose at a distance R from the center of the sphere whose radius is r_0 ($R > r_0$) is

$$D_s(R, r_0) = \frac{r_0}{R} [D_{p1}(R - r_0, \infty) - D_{p1}(R + r_0, \infty)] \quad (34)$$

The quantities in the brackets are the doses to be expected at distances of $R - r_0$ and $R + r_0$ from infinite plane sources of the same surface source strength.

If the attenuation length for the plane source data is sufficiently small in comparison with the diameter of the sphere, then the second term in the brackets can be ignored and

$$D_s(R, r_0) \cong \frac{r_0}{R} D_{p1}(R - r_0, \infty) \quad (35)$$

5.17 Plane to Cylindrical Shell Source. For conditions similar to the previous transformation, if the source is spread on an infinitely long cylinder of radius r_0 , the dose at a distance r from the cylinder axis is

$$D_c(r, r_0) \cong \sqrt{\frac{r_0}{R}} D_{p1}(R - r_0, \infty) \quad (36)$$

* Hurwitz transformation; for derivation see Ref. 15, part I.

5.2 Transformations for Surface Sources in Homogeneous Shields with Partially Specified Attenuation Functions

It is possible to extend the transformation geometry somewhat further if some assumption is made about the form of the attenuation kernel. The form of the attenuation function is unspecified for a distance z from the detector to the nearest source element, but for distances $R > z$ to other source elements the increased attenuation is assumed to be a pure exponential with a relaxation length λ , which can be taken from data as described by Eq. (30). Thus

$$G(R) \cong G(z)e^{-(R-z)/\lambda} \quad (37)$$

5.21 Quadric Sources. If the unit strength per unit area isotropic source is assumed to be spread uniformly on a quadric surface tangent to the XY plane (Fig.

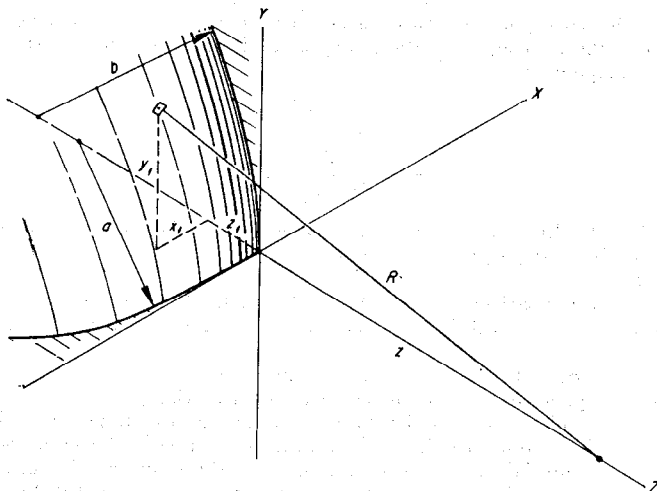


FIG. 10. Geometry for quadric surface source and homogeneous shield.

10), the equation describing the source surface near the origin is

$$z_1 \approx -\frac{1}{2} \left[\frac{(x_1)^2}{a} + \frac{(y_1)^2}{b} \right] \quad (38)$$

where x_1, y_1, z_1 = coordinates of curved source surface

a = radius of curvature in XZ plane

b = radius of curvature in YZ plane

The dose at the detector is then given by

$$D_q(z, a, b) \approx 2\pi s G(z) \left[\frac{1}{\left(\frac{1}{\lambda z} + \frac{1}{\lambda a}\right)^{1/2} \left(\frac{1}{\lambda z} + \frac{1}{\lambda b}\right)^{1/2}} + \frac{1}{2a^2 \left(\frac{1}{\lambda z} + \frac{1}{\lambda a}\right)^{3/2} \left(\frac{1}{\lambda z} + \frac{1}{\lambda b}\right)^{1/2}} \right. \\ \left. + \frac{1}{2b^2 \left(\frac{1}{\lambda z} + \frac{1}{\lambda a}\right)^{1/2} \left(\frac{1}{\lambda z} + \frac{1}{\lambda b}\right)^{3/2}} \right] \quad (39)$$

For $a, b, \gg \lambda$,

$$D_q(z, a, b) = 2\pi s G(z) \frac{1}{\left(\frac{1}{\lambda z} + \frac{1}{\lambda a}\right)^{1/2} \left(\frac{1}{\lambda z} + \frac{1}{\lambda b}\right)^{1/2}} \quad (39a)$$

For a derivation of this expression see Welton and Blizard.²⁵

Special Cases. For the special case of a plane surface source, $a, b \rightarrow \infty$ and

$$D_{p1}(z, \infty) = 2\pi z \lambda G(z) \quad (39b)$$

This is directly comparable to Eq. (27). For a spherical surface source, $a = b = r$, and for $r \gg \lambda$,

$$D(z, r) \cong 2\pi \lambda G(z) \frac{zr}{z+r} \quad (39c)$$

The same result can be found from combination of Eqs. (27) and (34).

5.3 Leakage Flux from Volume-distributed Sources

For a self-attenuating medium containing sources, the leakage can usually be satisfactorily calculated using first-flight methods. First flight will not give satisfactory answers when there is little attenuation per collision in the medium (as with diffusing thermal neutrons) or when the sources are concentrated largely in regions far from the source-shield boundary. However, for most neutron shielding calculations it is desired to determine the leakage of the penetrating component, and for this purpose either first-flight or exponential attenuation with removal cross sections is adequate.

In the foregoing paragraphs the use of surface distributions of sources has been discussed. These, with the attenuation kernels obtainable from Arts. 1 and 3, enable the calculation of shield performance. It remains to determine surface distributions which are equivalent to the volume sources such as reactor cores.

5.31 Uniformly Distributed Sources. At the surface of a volume containing uniformly distributed sources the leakage flux as a function of angle to the surface normal is

$$l(\theta) = \frac{p\lambda_c}{4\pi} \cos \theta \quad (40)$$

where θ = angle to the surface normal

$l(\theta)$ = leakage rate (of photons or neutrons) per unit area of source volume surface, per unit solid angle about a direction at an angle θ to the normal, $\text{cm}^{-2} \text{sec}^{-1}$

p = source strength, particles per unit volume per unit time, $\text{cm}^{-3} \text{sec}^{-1}$

λ_c = relaxation length in the source-containing material (core) for the radiation
 = $(\Sigma_r)^{-1}$, when Σ_r = macroscopic removal cross section for the core, cm^{-1} ,
 when fast neutrons are considered
 = $(\mu)^{-1}$, where μ = total linear attenuation coefficient for the core, cm^{-1} ,
 when γ rays are considered.

It is required that λ_c be small compared with the source dimensions and the local radius of curvature of the source-shield interface. The total leakage per unit area of surface is

$$\begin{aligned} L &= \int_{\theta=0}^{\pi/2} l(\theta) d\Omega \\ &= \frac{p\lambda_c}{4} \end{aligned} \quad (41)$$

This expression is useful when it is necessary to calculate the total heating, for example, of escaping γ rays, or the total escape of neutrons for purposes of obtaining a capture γ -ray source.

For shields it is necessary to calculate the leakage of the most important components of radiation. With thick shields especially, those neutrons or photons that penetrate are generally those that leave the surface in directions close to the normal. Consequently, the *equivalent isotropic surface source* is chosen to match the leakage flux in the normal direction [$\theta = 0$, Eq. (40)]

$$s_{eq} \cong p\lambda_c \quad (42)$$

where s_{eq} is that isotropic surface source, particles per square centimeter per second, which, if placed at the interface between the volume source and shield, gives the same dose at the shield exterior. It is here assumed that this source gives the same radiation per unit solid angle about the normal direction.

In case the dimensions of the volume source are not large compared with λ_c , a correction may be made on the basis of a simple integration over the interior points of the source volume. For very thin source regions,

$$s_{eq} \approx ph \quad (42a)$$

where h is the thickness of the source region in centimeters, and it is small compared with λ_c .

Corrections for curved surfaces, such as spherical source volumes, are in general small. The expression for the dose from a sphere of volume source density p becomes²⁶

$$D_{SV}(R, r_0) = \frac{\lambda_c p r_0 - \lambda_c}{s} \frac{D_{p1}(R - r_0, \infty)}{R} \quad (43)$$

where R = distance from center of sphere to receptor, cm

r_0 = radius of sphere, cm

s = source strength for plane data, $D_{p1}(R - r_0, \infty)$, cm^2/sec

This is to be compared with Eq. (35), from which it is seen that the equivalent surface source is very nearly $p\lambda_c$. The correction from r_0/R to $(r_0 - \lambda_c)/R$ takes into account that the surface is curved away from the receptor.

For small spherical cores, that is, $r_0 \ll \lambda_c$, a situation encountered in calculating γ rays from a small low-density reactor core, the dose is given by

$$D_{SV}(R, r_0) \cong \frac{2}{3} \frac{r_0^2 p}{R \lambda_c s} D_{p1}(R - r_0, \infty) e^{-\tau_0 \lambda_c} \quad (44)$$

For this same case the dose can be determined also in terms of the kernel directly:

$$D_{SV}(R, r_0) \cong 2\pi p R G(R) \left[R r_0 - \left(\frac{R^2 - r_0^2}{2} \right) \ln \left(\frac{R + r_0}{R - r_0} \right) \right] \quad (45)$$

If $r_0 \ll R$ and $r_0 \ll \lambda_c$,

$$D_{SV}(R, r_0) = \frac{4}{3} \pi r_0^3 p G(R) \quad (46)$$

The last equation follows from the fact that the total source $S = \frac{4}{3} \pi r_0^3 p$.

5.32 Nonuniformly Distributed Sources. In case the sources are not distributed uniformly over the volume, an integration is required. In this case,

$$D = \int_{\text{vol}} p(R_1) G(R_1, R) dV \quad (47)$$

where $G(R_1, R)$ is the attenuation for a point source a distance $R + R_1$ away, the distance R being measured in the shield and R_1 in the source-laden volume (e.g., reactor core).

For a strongly attenuating source volume, i.e., $r_0 \gg \lambda_c$, knowledge of the variation in source density near the boundary is adequate to make proper adjustments to the foregoing results. Thus, if the source density is given by

$$p(x) = p_0 + p_1 x \quad (48)$$

where p_0 = constant source strength term, $\text{cm}^{-3} \text{sec}^{-1}$

p_1 = first derivative of source term with respect to distance from surface, $\text{cm}^{-4} \text{sec}^{-1}$

x = normal distance from surface, measured inward, cm

then the leakage per unit surface area, per unit solid angle about a direction, at an angle θ to the normal, is

$$l(\theta) = \frac{p_0 \lambda_c \cos \theta}{4\pi} + \frac{p_1 \lambda_c^2 \cos^2 \theta}{4\pi} \quad (49)$$

The total leakage for this case is

$$\begin{aligned} L &= \int_{\theta=0}^{\pi/2} l(\theta) d\Omega \\ &= \frac{p_0\lambda_c}{4} + \frac{p_1\lambda_c^2}{6} \end{aligned} \quad (50)$$

The equivalent isotropic surface source is

$$s_{eq} = p_0\lambda_c + p_1\lambda_c^2 \quad (51)$$

5.4 Approximations for γ -ray Build-up Factors

In calculations of doses from source arrays, which usually involve integrations, it is convenient to approximate the build-up factors by an analytic function. The simplest of these is an exponential. The effective removal cross section concept for fast neutrons implies an exponential build-up factor. It has been demonstrated^{9,27} that build-up factors for γ rays can be well approximated by a sum of two exponential functions, as follows:

$$B(\mu t) = Ae^{-\alpha_1\mu t} + (1 - A)e^{-\alpha_2\mu t} \quad (52)$$

where $B(\mu t)$ = build-up factor, either for dose or energy absorption, for a given attenuating medium, such as water, iron, lead, or concrete, for a given energy per photon in the source. The use of this factor, which is dimensionless, is described in Art. 1

A, α_1, α_2 = constants which make Eq. (52) give the same build-up factors as are given in the tables of Art. 1

μ = total linear attenuation coefficient, cm^{-1} , from Table 1

t = thickness of attenuating material, cm

The advantage of using this mathematical form for the build-up factor is that it entails no extra complication in the calculation of dose from an array of sources. The parameters for the dose build-up factors in water, concrete, iron, and lead are given in Table 19.

5.5 Formulas for Flux in Various Source-Shield Geometries

If the algebraic form of the attenuation function is known, it may be possible to perform the integration at once over the source distribution. The simplest attenuation function (or kernel) is that with exponential attenuation and unitary build-up factor. For this,

$$G(R, t) = \frac{e^{-\mu t}}{4\pi R^2} \quad (53)$$

If *removal cross sections for fast neutrons* are used, then μ is, of course, just the macroscopic removal cross section and the build-up factor is taken to be unitary. This equation gives the current (of photons or neutrons) at a distance R from a source of unit strength with an interposed shield of thickness t and attenuation coefficient μ . If the approximations to γ -ray build-up factors^{9,27} are to be used, then the attenuation kernel would be

$$G(R, t) = \frac{Ae^{-(1+\alpha_1)\mu t} + (1 - A)e^{-(1+\alpha_2)\mu t}}{4\pi R^2} \quad (54)$$

If a *linear* build-up factor is to be used as is sometimes done for γ rays of energy just below the minimum in total cross section in light elements ($Z \gtrsim 26$),

$$G(R, t) = \frac{\mu t e^{-\mu t}}{4\pi R^2} \quad (55)$$

Better than the foregoing, because it gives the correct values for small μt , is a

Table 19. Values of A , $-\alpha_1$, and α_2 for Various Media and a Point Isotropic Source*

Energy, Mev	Value of constant			Worst error in fit, %
	A	$-\alpha_1$	α_2	
In Water Medium				
0.5	23	0.136		
1	11	0.104	0.028	
2	6.4	0.076	0.092	
4	4.5	0.055	0.1165	
6	3.55	0.0495	0.124	
8	3.05	0.045	0.128	
10	2.7	0.042	0.13	
In Ordinary Concrete Medium				
0.5	12.5	0.111	0.01	
1	9.9	0.088	0.029	
2	6.3	0.068	0.058	
4	3.9	0.059	0.079	
6	3.1	0.0585	0.083	
8	2.7	0.057	0.0855	
10	2.6	0.05	0.0835	
In Lead Medium				
0.5	1.65	0.032	0.296	-1.5
1	2.45	0.045	0.178	-3.9
2	2.60	0.071	0.103	+4.9
3	2.15	0.097	0.077	+5.0
4	1.65	0.123	0.064	+3.8
5.1097	1.20	0.152	0.059	-3.1
6	0.96	0.175	0.059	-3.9
8	0.67	0.204	0.067	+5.2
10	0.50	0.214	0.08	-3.3
In Iron Medium				
0.5	10	0.0948	0.012	6.8
1	8.0	0.0895	0.04	8.0
2	5.5	0.0788	0.07	5.9
4	3.75	0.075	0.082	6.25*
6	2.9	0.0825	0.075	4.95
8	2.35	0.0883	0.0546	2.8
10	2.0	0.095	0.0116	1.85

* SOURCE: Ref. 9, pp. 416-423.

combination of the unitary and linear build-up factors,

$$G(R,t) = \frac{(1 + \mu t)e^{-\mu t}}{4\pi R^2} \quad (56)$$

Somewhat more general than Eq. (56) is

$$G(R,t) = \frac{(1 + k\mu t)e^{-\mu t}}{4\pi R^2} \quad (57)$$

where k is a constant to be chosen for best fit to the actual kernel.It has been shown^{*,28} that for heating calculations with γ rays

$$k \cong \frac{\mu - \mu_a}{\mu_a} \quad (57a)$$

* Derivation given in Ref. 17, vol. 1, chap. 2.7.

This formula gives results between $\frac{2}{3}$ and $\frac{3}{2}$ of the correct build-up factors for $E \sim 2$ Mev in elements for which $Z \gtrsim 50$, up to $\mu t \lesssim 2$.

It should be borne in mind that the foregoing approximate formulas for build-up factors, with the exception of Eq. (54), are not to be preferred over those of Art. 1 except for convenience of calculation. They are not accurate and may lead to large errors for large attenuations.

All the attenuation kernels above can be described by a linear combination of Eqs. (53) and (55). Both γ rays and neutrons can be calculated by means of one or more kernels of the form of Eq. (53) [e.g., that of Eq. (54) for the γ -ray dose and Eq. (53) with removal cross sections for the fast-neutron dose], which is to say that the attenuation can be treated as if it were exponential. The constants for use of Eq. (54) are not all calculated, so that occasionally a kernel such as Eq. (57) is used. It will be assumed that in a shield of several regions the contribution of an element of source shall be described by Eq. (53), in which R is the linear separation between source element and receiver and μt is the sum of products of attenuation coefficients μ_1, μ_2, \dots , etc., for the several media and the distances in them, t_1, t_2, \dots , etc., measured along a straight ray between source and receiver ($\mu t = \mu_1 t_1 + \mu_2 t_2 + \dots$). This assumption is not conservative and may lead to significant error if the μ s vary greatly, as with lead and water γ -ray shields. Thus if the surfaces between the different media are not nearly perpendicular to the direction of radiation propagation, scattering will enable the radiation to take paths which, while longer, take less distance in the better attenuator and hence have less total attenuation. This effect of "short circuiting" has been studied experimentally²⁹ and theoretically³⁰ for the simple case of radiation obliquely incident on a slab shield. No simple calculational method of accounting for it is available. Conservative (high) estimates of the dose can be had by calculating μt for the minimum attenuation path, the path being a succession of straight rays in successive media.

For exponential attenuation [Eq. (53)], no "short circuiting," and isotropic detector, formulas for the flux are given below. Symbols used throughout the formulas are defined as follows:

ϕ = flux of photons or neutrons, $\text{cm}^{-2} \text{sec}^{-1}$ [for a point source of unit strength $\phi(R) = G(R)$; for distributions of sources, ϕ represents the result of integrating G over all sources]

S = source strength for a point source, sec^{-1}

s = source strength for a surface source, $\text{cm}^{-2} \text{sec}^{-1}$

p = source strength for a volume source, $\text{cm}^{-3} \text{sec}^{-1}$

Λ = source strength for a line source, $\text{cm}^{-1} \text{sec}^{-1}$

μ = attenuation coefficient for the shield, cm^{-1} (see previous paragraphs)

μ_c = attenuation coefficient for source-bearing material (core), cm^{-1}

t = shield thickness, cm

$$E_0(\mu t) = \frac{e^{-\mu t}}{\mu t} \quad \text{for } \mu t < 10 \quad (\text{see Figs. 11a-c})$$

$$E_n(\mu t) = (\mu t)^{n-1} \int_{\mu t}^{\infty} \frac{e^{-x}}{x^n} dx \quad \text{for } \mu t < 10 \quad (\text{see Figs. 11a-c})$$

$$= \frac{e^{-\mu t}}{\mu t} \left[1 - \frac{n}{\mu t} + \frac{n(n+1)}{(\mu t)^2} - \frac{n(n+1)(n+2)}{(\mu t)^3} + \dots \right] \quad \text{for } \mu t > 10$$

$$F(\theta, \mu t) = \int_0^\theta e^{-\mu t \sec \theta'} \sec \theta' d\theta' \quad \text{for } \mu t > 10 \quad (\text{see Figs. 12a-d})$$

5.51 Point Source. The flux beyond a slab shield due to a point source is given by

$$\phi(R) = SG(R, t) \quad (58)$$

$$= \frac{Se^{-\mu t}}{4\pi R^2} \quad (58a)$$

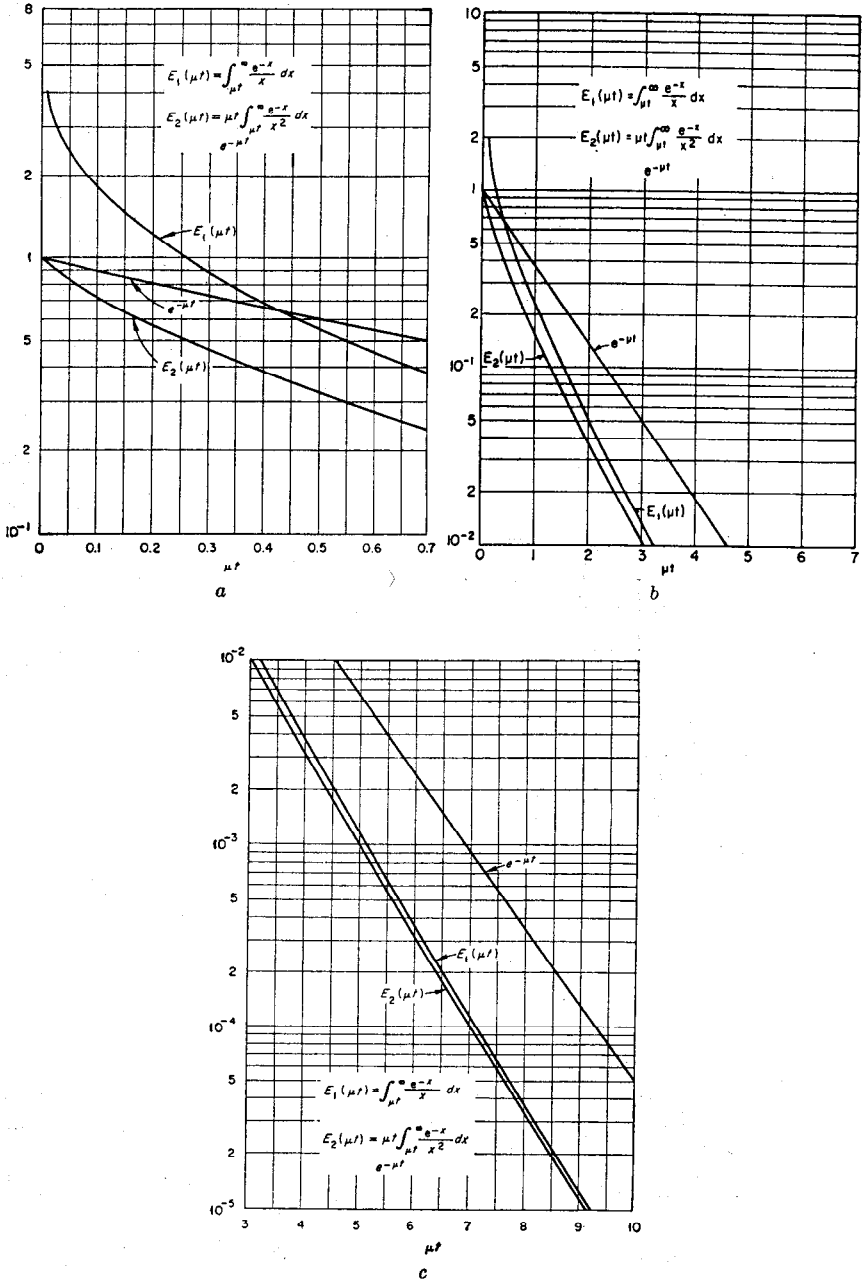


FIG. 11. $e^{-\mu t}$, $E_1(\mu t)$, and $E_2(\mu t)$: a. $\mu t = 0$ to 0.7 ; b. $\mu t = 0$ to 7 ; c. $\mu t = 3$ to 10 .

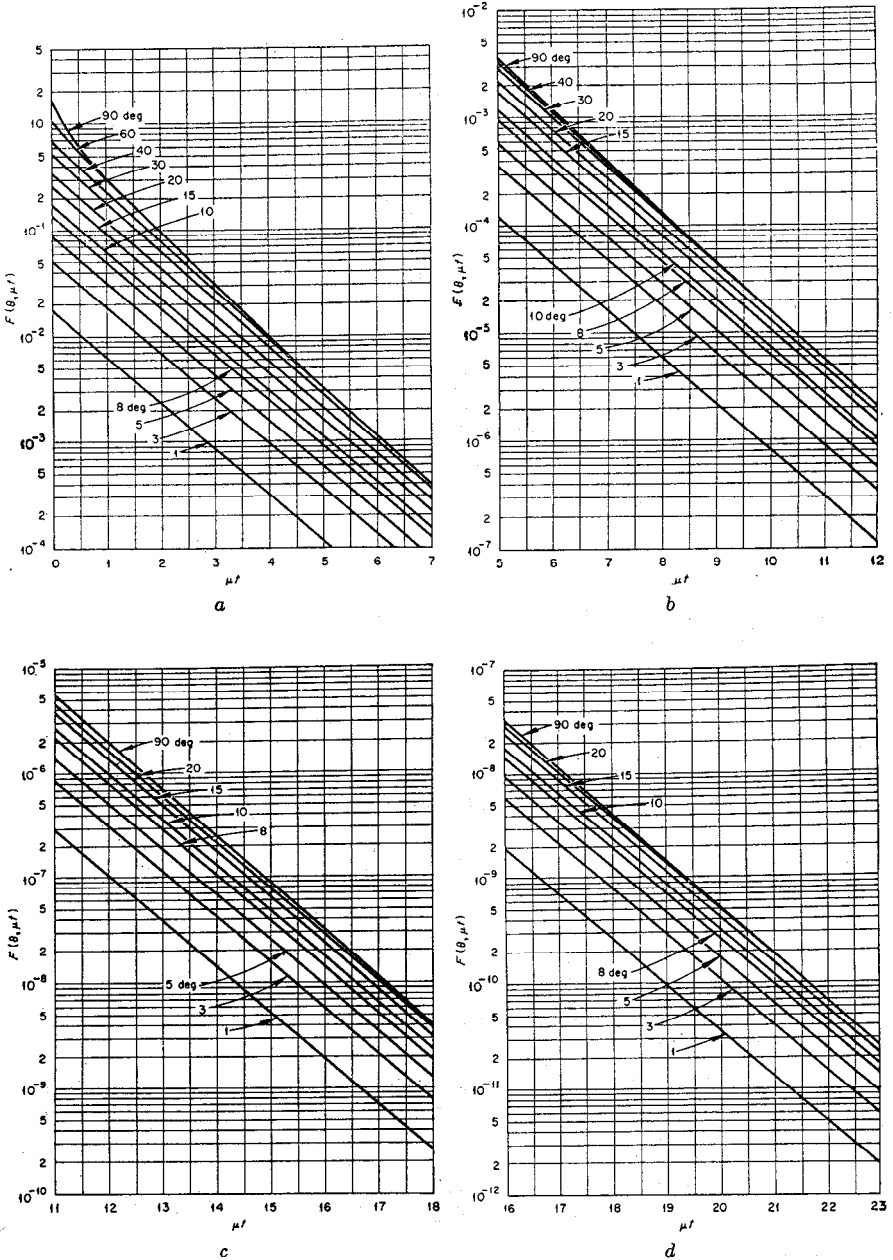


FIG. 12. The function $F(\theta, \mu\tau)$: a. $\mu\tau = 0$ to 7; b. $\mu\tau = 5$ to 12; c. $\mu\tau = 11$ to 18; d. $\mu\tau = 16$ to 23.

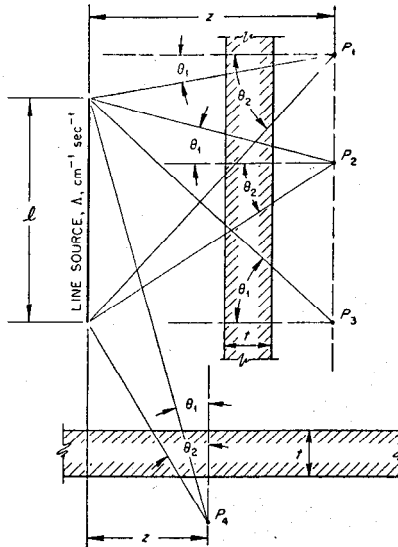


FIG. 13. Geometry for line source and slab shield.

5.52 Line Source. At P_1 and P_4 beyond a slab shield (Fig. 13), the flux due to a line source is given by

$$\phi = \frac{\Lambda}{4\pi z} [F(\theta_2, \mu t) - F(\theta_1, \mu t)] \quad (59)$$

At P_2 ,

$$\phi = \frac{\Lambda}{4\pi z} [F(\theta_1, \mu t) + F(\theta_2, \mu t)] \quad (59a)$$

At P_3 ,

$$\phi = \frac{\Lambda}{4\pi z} F(\theta_1, \mu t) \quad (59b)$$

5.53 Disk Source. For a point at distance z (Fig. 14) along the axis of a disk source and beyond a shield of thickness t (i.e., $t < z$),

$$\phi = \frac{s}{2} \left\{ E_1(\mu t) - E_1 \left[\mu t \sqrt{1 + \left(\frac{a}{z} \right)^2} \right] \right\} \quad (60)$$

5.54 Infinite Plane Source. The flux beyond a slab shield due to an infinite plane source is given by

$$\phi = \frac{s}{2} E_1(\mu t); \quad \phi \cong \frac{se^{-\mu t}}{2\mu t} \quad \text{for } \mu t \gg 1 \quad (61)$$

The outbound particle current density is

$$I = \frac{s}{2} E_2(\mu t) \cong \frac{s}{2} \frac{e^{-\mu t}}{\mu t} \quad \text{for } \mu t \gg 1 \quad (62)$$

5.55 Thick Slab Volume Source. If the source is distributed throughout a thick slab volume the flux beyond the slab shield is given by

$$\phi = \frac{p}{2\mu_c} E_2(\mu t) \cong \frac{p}{2\mu_c} \frac{e^{-\mu t}}{\mu t} \quad (63)$$

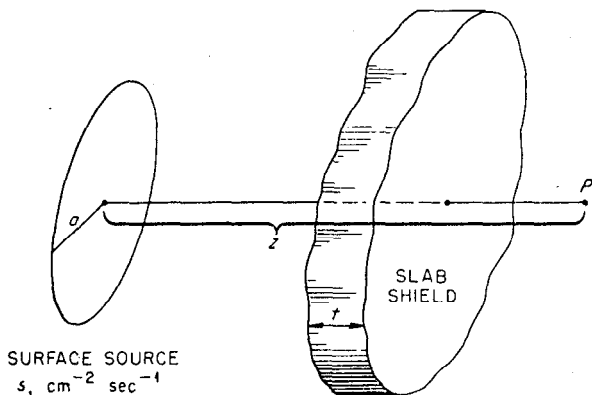


FIG. 14. Geometry for disk source and slab shield.

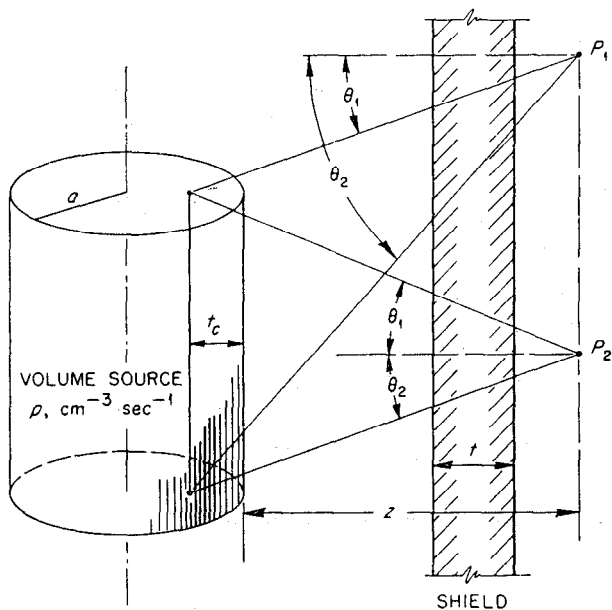


FIG. 15. Geometry for cylindrical volume source and slab shield at side.

and the outbound current density is

$$\begin{aligned}
 I &= \frac{1}{2\mu_c} E_2(\mu t) \\
 &\cong \frac{1}{2\mu_c} \frac{e^{-\mu t}}{\mu t}
 \end{aligned}
 \tag{64}$$

5.56 Cylindrical Volume Source with Shield at Side. To obtain flux from sources distributed uniformly in a cylinder of attenuating material (μ_c , cm^{-1}), with a slab shield exterior and parallel to the cylinder axis (Fig. 15), it is necessary to obtain a

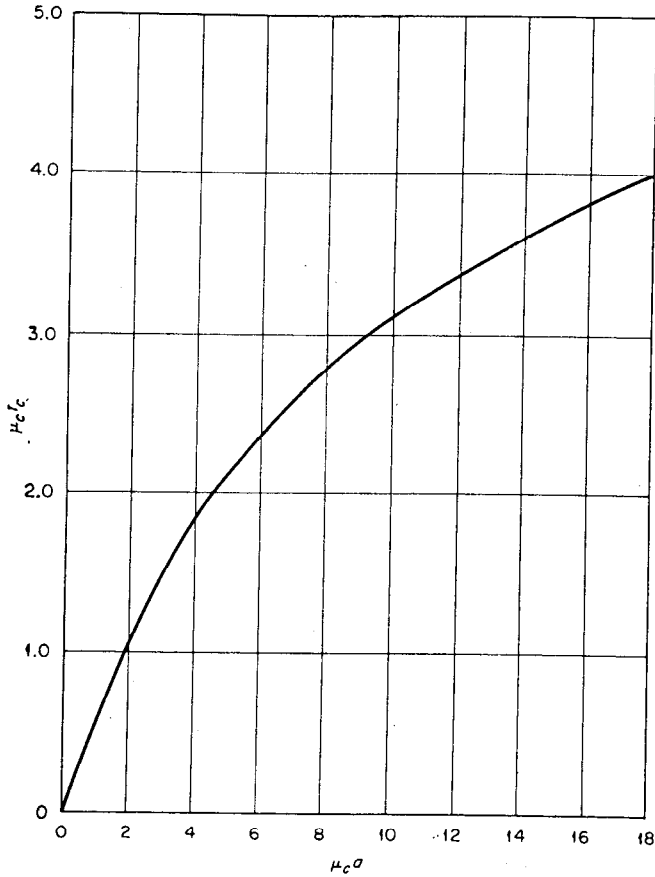


Fig. 16. Self-absorption exponent, $\mu_c t_c$, of a cylinder as a function of its radius, a , for $z/a \geq 10$.

self-absorption distance t_c from Figs. 16 to 18 and to use the $F(\theta, \mu t)$ attenuation functions. At P_1 (Fig. 15),

$$\phi = \frac{pa^2}{4(z + t_c)} [F(\theta_2, \mu t + \mu_c t_c) - F(\theta_1, \mu t + \mu_c t_c)] \quad (65)$$

at P_2 ,

$$\phi = \frac{pa^2}{4(z + t_c)} [F(\theta_2, \mu t + \mu_c t_c) + F(\theta_1, \mu t + \mu_c t_c)] \quad (65a)$$

Note: To obtain $\mu_c t_c$, use Fig. 16 if $z/a \geq 10$. If $z/a < 10$, use Fig. 17 to obtain $\mu_c t_c/m$ and then obtain m from Fig. 18.

5.57 Cylindrical Volume Source with Shield at End. For this geometry upper and lower limits, based on truncated cones, are given for the flux. The upper limit is for the upper truncation surface equal to the actual cylinder base. The lower limit is for the truncated cone with lower base equal to the actual cylinder base (Fig. 19). The upper limit is

$$\phi_u = \frac{p}{2\mu_c} \left\{ E_2(\mu t) - E_2(\mu t + \mu_c h) + \frac{E_2[(\mu t + \mu_c h) \sqrt{1 + (a/z)^2}]}{\sqrt{1 + (a/z)^2}} - \frac{E_2[\mu t \sqrt{1 + (a/z)^2}]}{\sqrt{1 + (a/z)^2}} \right\} \quad (66)$$

The lower limit is the same expression with z replaced by $(z + h)$. Note: for $\mu_c h > 3$, the second and third E functions in the above expression can be neglected with an error of about 5 per cent or less.

5.58 Spherical Volume Source. For the geometry in Fig. 20,

$$\phi = \frac{2}{3} pa \left\{ E_1(\mu t + \mu_c t_c) - E_1 \left[(\mu t + \mu_c t_c) \sqrt{1 + \left(\frac{a}{z + t_c} \right)^2} \right] \right\} \quad (67)$$

where $\mu_c t_c$ is found from Figs. 21 and 22 using a calculated value of $\mu_c a$.

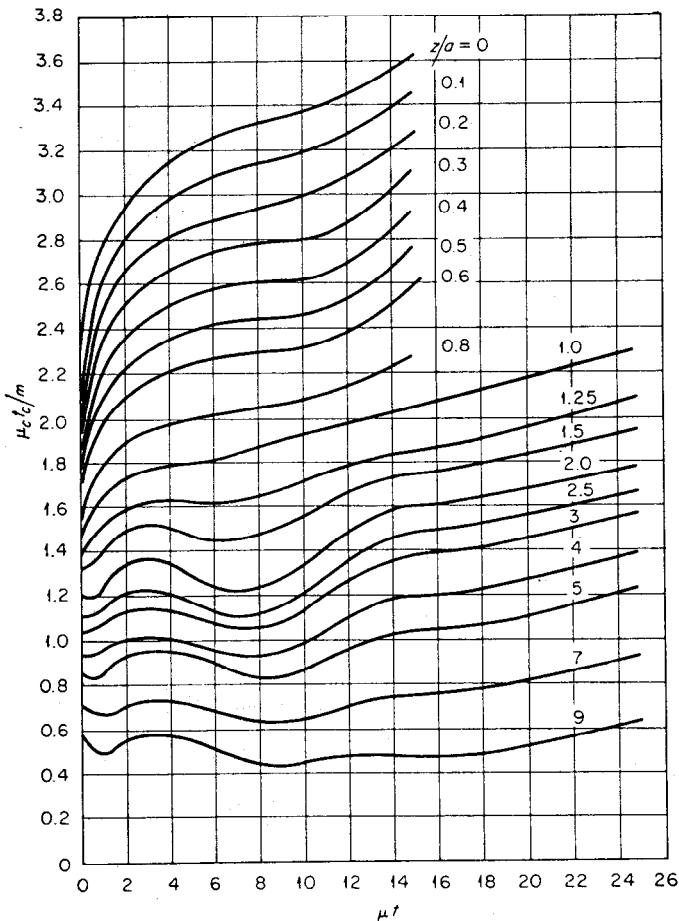


Fig. 17. Self-absorption exponent divided by self-absorption parameter, $\mu_c t_c / m$, as a function of μt for $z/a < 10$.

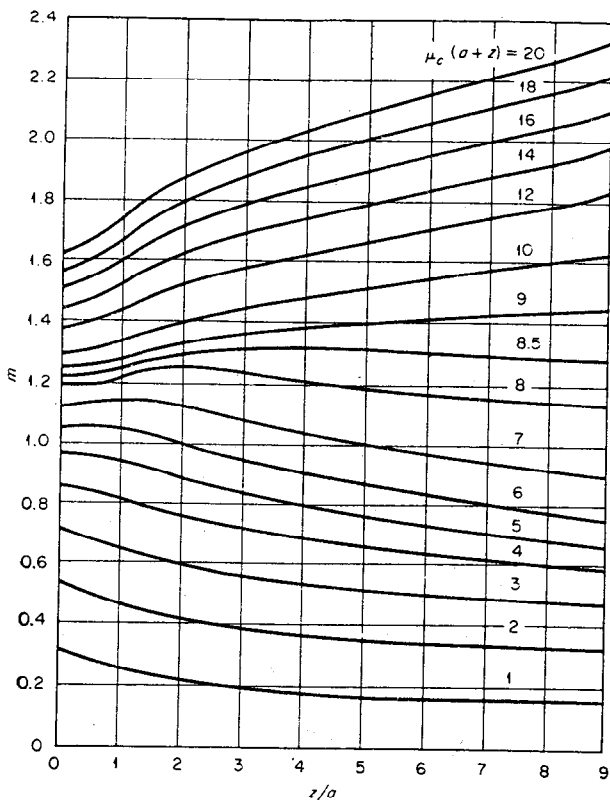


Fig. 18. Self-absorption parameter, m , for a cylinder as a function of its radius, a , for $z/a < 10$.

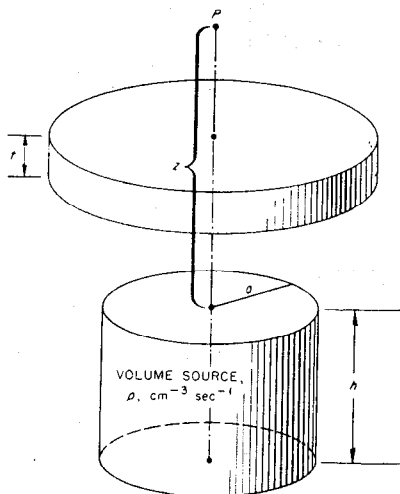


Fig. 19. Geometry for cylindrical volume source and slab shield at end.

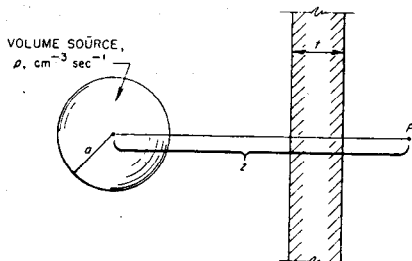


Fig. 20. Geometry for spherical volume source and slab shield.

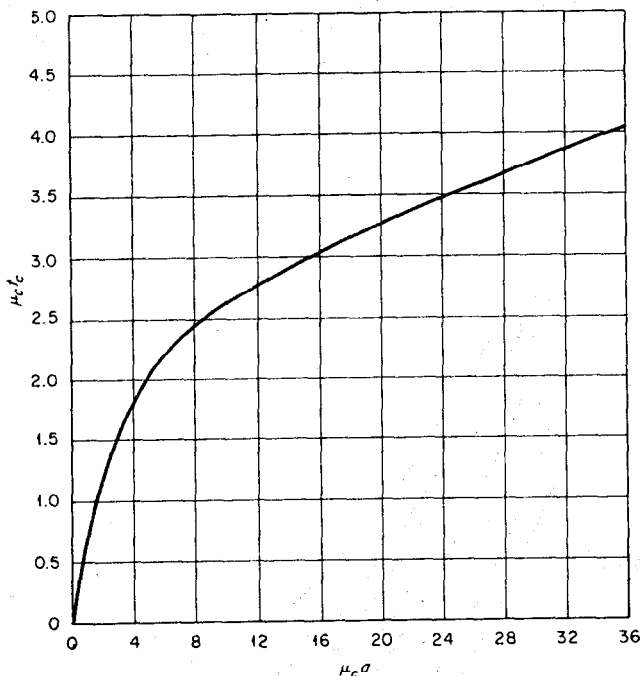


FIG. 21. Self-absorption exponent, $\mu_c c$, of a sphere as a function of its radius, a , multiplied by μ_c for $2/a \geq 1$.

6 SHIELD MATERIALS

6.1 Criteria for Selection of Shield Materials

Choice of shield materials varies drastically with application, as does the relative importance of the several criteria. The most important commonly used criteria are radiation attenuation, ease of heat removal, resistance to radiation damage, expense, and structural strength.

6.11 Attenuation. 1. *Neutrons.* The attenuation of fast neutrons is described in Art. 3. The removal cross section is the best criterion, subject to the limitations due to diffusion of intermediate neutrons as discussed there. The lightest shields are usually hydrogenous, whereas the thinnest shields will contain a large volume fraction of iron, copper, or some other material in which the atoms are closely spaced.

2. *Gamma Rays.* The attenuation of γ rays is described in Art. 1. In general, the high-atomic-number elements are the best γ -ray shields, except that hydrogen itself is good on a weight basis. However, the build-up of scattered γ rays in hydrogen is high and no really dense forms exist, so that this element is not often considered for γ -ray shields.

3. *Capture γ -ray Suppression.* Gamma rays produced within the shield by neutrons are often serious sources of radiation. Capture γ rays may be suppressed by the elements boron, lithium, and nitrogen, as shown in Art. 2 (Table 10). Of these, the first two excel because of their large capture cross sections.

6.12 Heat Removal. It is often necessary to remove heat from the inner layers of a shield. For this reason the shield in those regions must have good heat conductivity or must be capable of being circulated to a heat exchanger. If the exchanger

is not shielded, the circulated material must not become radioactive. Fixed shields may be steel or copper, cooled by water, helium, or nitrogen, for example. The water will become activated, however, by fast neutrons, so that the heat exchanger must be shielded. Shields which are circulated may be water, molten lead or bismuth, or an alloy of the two.

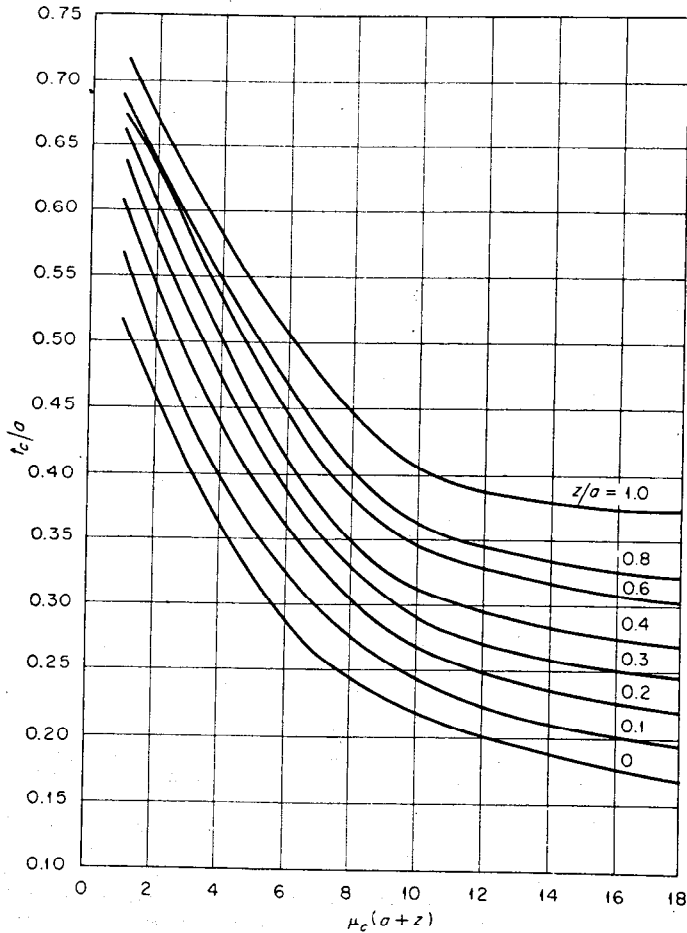


FIG. 22. Ratio of self-absorption distance to radius, t_c/a , for a sphere as a function of distance to its center, $z+a$, multiplied by μ_c for $z/a < 1$.

6.13 Radiation-damage Resistance. It is, of course, essential that the radiation which the shield attenuates does not have a significantly deleterious effect on the shield itself, impairing either its structural integrity or its ability to attenuate. This problem is most acute in the innermost layers in which the radiation is greatest. In general, the metals are most resistant to damage, although they are subject to some rearrangement within the crystal lattices which affect their strength. Concretes seem to hold up well, although if heated they will lose water of crystallization, becoming somewhat weaker and less effective in neutron attenuation. Hydrogenous

materials, such as the plastics and wood, are particularly tender, often undergoing gross changes. Simple molecules such as H₂O or NH₃ seem to be exceptions in that recombination can be effected and the decomposition products can be removed with no impairment of the attenuating property of the residual material. Several review articles on radiation damage have been published.^{31,32} See Secs. 10-4 and 10-5.

6.14 Expense. In many shielding problems expense is the paramount consideration. In this case a careful balance must first be made between the intrinsic cost of the shield and the effect of shield size and configuration on other aspects of the installation, such as building size, support structure, etc. In the choice of the shield material itself, transportation costs should be carefully considered. Local material such as natural minerals (e.g., barytes in east Tennessee) and waste material (e.g., steel scrap) should be evaluated as aggregates to be used with portland cement. Earth itself provides a fair shield. Water is an excellent shield if large thicknesses can be tolerated, and the thickness can be strongly reduced by adding a layer of lead or steel for γ -ray attenuation.

6.2 Shielding Properties of Specific Materials

The macroscopic removal cross sections for several hydrogen-containing materials used for neutron attenuation are listed in Table 20. The attenuation coefficients for some of the heavy elements, particularly effective as γ -ray shields, are given in Table 21. Table 22 illustrates the method of computing both the neutron and the γ -ray shielding properties of a mixture. For this example the effectiveness of each element in two different concretes, portland and barytes, is computed.

Table 20. Macroscopic Neutron Removal Cross Sections for Materials Containing Hydrogen

(a)

Compound	Chemical formula	Density, g/cm ³	N _H *	Σ_r/ρ , cm ² /g†	Σ_r , cm ⁻¹
Ammonia.....	NH ₃	0.771 (78%)	8.18	0.144	0.111
Lithium borohydride.....	LiBH ₄	0.686	7.58	0.165	0.113
Lithium hydride.....	LiH	0.820	6.21	0.152	0.125
Water.....	H ₂ O	1.00	6.69	0.100	0.100

(b)

Material	Assumed chemical formula	Density, g/cm ³	N _H *	Σ_r/ρ , cm ² /g†	Σ_r , cm ⁻¹
Fuel oil.....	CH _{1.6}	0.89	6.4	0.106	0.095
Gasoline.....	C ₈ H ₁₈	0.71-0.73	6.7	0.124	0.093
Natural rubber.....	(C ₅ H ₈) _n	0.92	6.5	0.106	0.098

* N_H is the atomic density of hydrogen, 10²² atoms/cm³.
 † Σ_r/ρ is the macroscopic removal cross section divided by the compound density (see Art. 3). For purposes of rough comparison, hydrogen is assigned 1 barn.

Tables 23 to 27 give data on cost, composition, and property of high-density concrete taken from an article by H. S. Davis.³³

Material cost in Table 25 includes costs for raw material, transportation, processing, and handling. Cost can be adjusted for local prices using the mix data. Costs increase with density and water content. Limonite, combined with barite, magnetite, or steel aggregate, raises fixed water content to about 5 per cent. If the amounts of

Table 21. Attenuation Coefficients for γ -ray Shield Materials

Element	ρ , g/cm ³	μ/ρ , cm ² /g*					μ , cm ⁻¹				
		0.5 Mev	1 Mev	2 Mev	3 Mev	6 Mev	0.5 Mev	1 Mev	2 Mev	3 Mev	6 Mev
		Iron.....	7.78	0.0840	0.0598	0.0422	0.0359	0.0305	0.653	0.465	0.329
Tungsten.....	19.3	0.131	0.0655	0.0432	0.0400	0.0426	2.528	1.263	0.835	0.772	0.823
Mercury.....	13.5	0.147	0.0692	0.0451	0.0411	0.0441	1.993	0.939	0.611	0.557	0.598
Lead.....	11.3	0.152	0.0703	0.0456	0.0413	0.0445	1.718	0.794	0.515	0.466	0.503
Bismuth.....	9.8	0.156	0.0714	0.0461	0.0417	0.0449	1.53	0.700	0.455	0.409	0.440
Uranium.....	18.7	0.185	0.0779	0.0483	0.0435	0.0471	3.46	1.458	0.904	0.814	0.882

* Mass attenuation coefficient, i.e., total linear attenuation coefficient divided by density (see Art. 1).

Table 22. Composition and Properties of Concretes for Shielding
(Illustrating method of computation of attenuation coefficients for mixtures)

Element	Atomic weight, A	ρ_c , density in concrete, g/cm ³	Neutron attenuation*		γ -ray attenuation for 6 Mev†	
			Σ_r/ρ , cm ² /g	Σ_r , cm ⁻¹	μ/ρ , cm ² /g	μ , cm ⁻¹
Ordinary (Portland) Concrete						
O	16.0	1.103	0.041	0.0452	0.0255	0.0282
Si	28.06	0.2815	0.0295	0.0083	0.0279	0.0079
Al	26.97	0.0330	0.0301	0.0010	0.0266	0.0009
Fe	55.85	0.0183	0.0200	0.0004	0.0305	0.0006
Ca	40.08	0.7712	0.024	0.0185	0.0302	0.0233
C	12.01	0.0761	0.050	0.0038	0.0246	0.0019
Na	23.00	0.0116	0.033	0.0004	0.0255	0.0003
K	39.10	0.0079	0.0245	0.0002	0.0289	0.0002
H	1.0	0.0250	0.602	0.0150	0.0449	0.0011
Mg	24.32	0.0426	0.032	0.0014	0.0267	0.0011
Total		2.37		0.0942		0.0655
Barytes Concrete						
Ba	137.36	1.470	0.0124	0.0182	0.0367	0.0539
O	16.0	1.090	0.041	0.0447	0.0255	0.0278
S	32.07	0.348	0.0275	0.0096	0.0287	0.0100
Fe	55.85	0.307	0.0200	0.0061	0.0305	0.0094
Ca	40.08	0.159	0.024	0.0038	0.0302	0.0048
Si	28.06	0.061	0.0295	0.0018	0.0279	0.0017
Al	26.97	0.020	0.0301	0.0006	0.0266	0.0005
H	1.0	0.015	0.602	0.0090	0.0449	0.0007
Mg	24.32	0.013	0.032	0.0004	0.0267	0.0003
Na	23.0	0.005	0.033	0.0002	0.0255	0.0001
Mn	54.93	0.003	0.0202	0.0001	0.0294	0.0001
Total		3.49		0.0945		0.1093

* Σ_r/ρ is the macroscopic removal cross section divided by the compound density (see Art. 3).

† μ/ρ is the mass attenuation coefficient, i.e., total linear attenuation coefficient divided by density (see Art. 1).

Table 23. Concrete Aggregates

Heavy aggregate	Source	Composition	Specific gravity*		Per cent by weight		Dollars/ton	
			Coarse pieces	Fine sand	Iron	Fixed water	FOB source	Processed at job†
Limonite-goethite‡	Mich.	2Fe ₂ O ₃ ·3H ₂ O	3.75	3.80	58	9	7	25-40
	Utah	Fe ₂ O ₃ ·H ₂ O	3.45	3.70	55	11	11-20	40-50
		Fe ₂ O ₄ , etc.	4.62	4.68	64	1	9	20-30
Magnetite.....	Nev.	Hydrous iron¶	4.30	4.34	60	2-5	7	18
Magnetite.....	Mont.	>92% BaSO ₄	4.20	4.24	1-10	0	18	22-30
Barite.....	Tenn.	>90% BaSO ₄	4.28	4.31	<1	0	19	30-40
Barite.....	Nev.	Fe ₃ P, Fe ₂ P, FeP	6.30	6.28	70	0	80	90
Ferrophosphorus.....	Tenn., Mo., Mont.							
Steel aggregate.....	Punchings, sheared bars	SAE standard	7.78	99	0	120	130
Steel shot.....	Chilled		7.50	98	0	120	130

* Material water saturated, with its surface dry.

† Processing charges include grinding and other operations to make the ore suitable for use in concrete. Freight charge of \$10/ton is included. Cost of grout sand is in italics.

‡ This ore occurs as a mixture of the two minerals.

¶ This ore is primarily magnetite, with some hematite (Fe₂O₃) and limonite.

source: H. S. Davis, *Nucleonics*, Ref. 33.

Table 24. Grouts

Type*	Grout sand	Sand/cement ratio		Water/cement weight ratio	Wet weight, lb/ft ²
		Weight	Volume		
S-270	No. 110 steel shot	3.75	1.58	0.35	270
S-250	No. 110 steel shot	3.30	1.39	0.35	250
M-170	Magnetite	2.13	1.04	0.55	170
B-155	Barite	1.49	1.10	0.54	155
L-146	Limonite	1.28	1.09	0.55	146

* Grout sands processed from heavy ores should have a fineness modulus of 1.0 to 1.5; the heavier the sand, the finer it must be to stay in suspension. Sands having 20 to 40 per cent finer than No. 200 screen may be used if tensile strength at high temperature is not important.

Each of the above grouts is pumpable; however, the metallic ones should not be pumped into large masses of aggregates. Grout S-250 may be pumped more easily than grout S-270.

source: H. S. Davis, *Nucleonics*, Ref. 33.

magnetite and limonite are varied, density can be varied from 175 to 250 lb/ft³, with corresponding fixed water content from 20 to 30 lb.

Natural-aggregate concretes cost 1 to 1.5¢/lb for materials. Using iron aggregate, densities from 240 to 425 can be obtained at 2 to 6¢/lb. This concrete can be justified only where space is at a premium.

The greatest potential cost savings are in simplifying form work, reducing labor, and using natural heavy aggregates rather than steel. Estimated costs at left show that usually form cost is over half the total cost. In the first three cases, temporary plywood forms were used, while permanent steel forms were used in the others.

On one job using elaborate steel forms cost breakdown was: 16 per cent, form fabrication; 20 per cent, materials other than aggregate; 30 per cent, labor at the site; 12 per cent, equipment; 15 per cent, steel aggregate; 7 per cent, limonite and magnetite aggregate. Limonite and magnetite are over 50 per cent of the volume of the concrete.

Table 25. High-density Concretes for Shielding

Concrete type	Weight, lb/ft ³	Material cost, dollars/ft ³	Compressive strength, psi ^a	Cement, lb/ft ³	Heavy aggregate: fine, lb/ft ³ ; coarse, lb/ft ^{3b}	Admixture ^c	Mix water, lb/ft ³	Water content, lb/ft ^{3d}		Grout type	Placement
								Min	Max		
A	410	25.40	3,000 (3)	16.8	#110 shot 63; punchings 324	I.A.	5.9	2.5	5.9	S-270	Puddled
B	346	18.40	3,000 (3)	20.6	Magnetite 44; punchings 270	I.A.	11.3	3.5	11.8	M-170	Prepacked
C	300	15.40	4,700 (3)	MO ^e	Ferrophosphorus 107; 161			~9.5	15.0		Conv.
D	300	12.05	3,870 (4)	24.1	Ferrophosphorus 92; 171		12.7	3.6	12.7		Conv.
E	300	11.90	5,000 (3)	19.8	Magnetite 42; magnetite + punchings 67 + 160	I.A.	10.9	4.1	12.0	M-170	Pre.
F	263	11.20	6,000 (3)	22.2	Limonite ^f 28; limonite + punchings 60 + 140	I.A.	12.2	13.0	21.9	L-146	Pre.
G	262	11.30	7,000 (3)	34.0	Limonite 65; shot No. 330 + 1320; 49 + 100	Plast.	13.5	12.3	20.9	Mortar	Conv.
H	262	7.75	5,350 (4)	23.7	Ferrophosphorus + barite 70 + 35; 70 + 50		12.8	3.6	12.8		Conv.
I	262	5.75	4,800 (3)	19.8	Magnetite 42; magnetite + punchings 122 + 67	I.A.	10.9	4.7	12.6	M-170	Pre.
J	244	2.55	5,000 (3)	17.5	Magnetite 37; 180	I.A.	9.7	4.8	11.9	M-170	Pre.
K	232	2.20	6,500 (3)	24.3	Magnetite 86; 110		11.5	5.7	13.5		Conv.
L	227	3.30	3,500 (3)	19.3	Barite 29; 168	I.A.	10.5	2.9	10.5	B-155	Pre.
M	222	3.05	6,000 (3)	19.3	Barite 86; 105		11.6	2.9	11.6		Conv.
N	219	2.10	6,500 (3)	24.9	Hydrous iron ore 82; 100	Plast.	12.0	9.2	17.5		Conv.
O	215	2.75	5,000 (3)	22.7	Limonite 29; limonite + magnetite 28 + 122	I.A.	12.5	10.9	20.0	L-146	Pre.
P	185	3.10	5,800 (1)	31.3	Limonite 62; 76	Plast.	15.4	17.1	27.8		Conv.
Q	154	0.50	8,800 (1)	31.3	Local sand 50; 61	Plast.	11.5	4.7	11.5		Conv.

^a Tested after number of months indicated in parentheses.

^b Where only one material is given, it is used for both fine and coarse aggregate.

^c Intrusion Aid, 1.5 per cent by weight of the portland cement, is added where shown. I.A. (Intrusion Aid) is a special grout admixture designed and used by Prepak Concrete Co., Cleveland, Ohio. Plast. (Plastiment) is a concrete densifier manufactured by Sika Chemical Corp., Passaic, N.J.

^d Maximum water content is water weight when concrete is wet. Minimum water content is amount left after drying at 85°C. Difference between maximum water content and amount of mix water added is water of crystallization held by aggregate. The difference between minimum water content and water of crystallization is water retained by the hardened cement paste.

^e This concrete is made using magnesium-oxychloride cement, made of 12.2 lb/ft³ of MgO powder and 19.8 lb of MgCl₂ solution.

^f Utah limonite is used except for mix P, which uses Michigan limonite.

source: H. S. Davis, *Nucleonics*, Ref. 33.

Table 26. Physical Properties of Concretes

Concrete*	Lb/fts	Bags/yd ³	Compressive strength, psi†	Rupture modulus, psi†	Elast. modulus (× 10 ⁻⁶)†	Ult. bond strength, psi†	Shrinkage, %	Expansion, in./in. (°F)	Specific heat, Btu/(lb)(°F)	Conductivity, Btu/(hr)(ft)(°F)	Diffusivity, ft ² /hr
Conv. (15)	153	~5.0	4,960	630	4.6	0.041	5.5	0.23	1.50	0.042
Q (16)	154	9.0	8,870	1,005	5.9	900	0.012				
P (16)	185	9.0	5,865	700	4.4	970	0.021				
O (17)	210	6.55	4,640	516	5.0	1,396	0.023	5.6	0.20	1.20	0.030
M (15)	226	5.1	6,130	445	4.3	0.029	10	0.157	0.884	0.025
L (15)	230	5.0	3,340	630	3.7	0.029	10	0.146	0.867	0.026
K' (17)	224	7.0	5,780	684	4.3	1,423	0.018	5.7	0.21	1.68	0.034
F (17)	273	6.55	3,180	406	5.4	1,266	0.013	5.9	0.18	2.75	0.056

* Concrete composition is similar to that given in table of concretes, except for K', which has 46-lb limonite and 0.6-lb fixed water per cubic foot. Conv. is Grand Coulee concrete. Placement method is given in Table 25. The limonite used was from Michigan; the barite was from Nevada; specific gravity of magnetite was 4.4.

† Strength values are for moist cured specimens, 28 days old.

SOURCE: H. S. Davis, *Nucleonics*, Ref. 33.

Table 27. Concrete Shield Costs

Concrete	Type	Cost, dollars/yd ³		Total cost/lb, cents
		Forms	Concrete	
Ordinary structural.....	45	25	1.7
Ordinary.....	Q	60	40	2.4
High density.....	K or N	100	120	3.7
High density.....	O	300	250	9.5
High density.....	F	600	500	15.5

SOURCE: H. S. Davis, *Nucleonics*, Ref. 33.

REFERENCES

1. Fano, U.: Gamma-ray Attenuation, *Nucleonics*, 11(1): 8 (August, 1953); 11(2): 55 (September, 1953).
2. Goldstein, H., and J. E. Wilkins: "Calculations of the Penetration of Gamma Rays," NYO-3075, June 30, 1954 (available from the Office of Technical Services, Department of Commerce, Washington).
3. "Reactor Handbook," Vol. I, chap. 2.3, Technical Information Service, U.S. Atomic Energy Commission, 1955.
4. Grodstein, Gladys White: "X Ray Attenuation Coefficients from 10 Kev to 100 Mev," *Natl. Bur. Standards Circ.* 583, April, 1957.
5. Davisson, C. M., and R. D. Evans: *Revs. Mod. Phys.*, 24: 79 (1952).
6. Nelms, A.: Graphs of the Compton Energy—Angle Relationship and the Klein-Nishina Formula from 10 Kev to 500 Mev, *Natl. Bur. Standards Circ.* 542.
7. Gamble, R. L.: "Prompt Fission Gamma Rays from Uranium 235," Dissertation, University of Texas, Austin, Tex., June, 1955.
- 8a. Hollander, J. M., I. Perlman, and G. T. Seaborg: Table of Isotopes, *Revs. Mod. Phys.*, 25: 469 (1953).
- b. Clark, F. H.: "Decay of Fission Product Gammas," NDA-27-39, Dec. 30, 1954.
- c. Moteff, John: "Fission Product Decay Gamma Energy Spectrum," APEX-134, June, 1953.
- d. Way, K., et al. "Nuclear Data," *Natl. Bur. Standards Circ.* 499 and Supplements 1 and 2.
- e. Supplements and Nuclear Data Compilations in NSA.
9. Rockwell, T. (ed.): "Reactor Shielding Design Manual," TID-7004, March, 1956.